

The published version of the paper " F. Luzi, E. Fortunati, D. Puglia, R. Petrucci, J.M. Kenny, L. Torre (2015) Study of disintegrability in compost and enzymatic degradation of PLA and PLA nanocomposites reinforced with cellulose nanocrystals extracted from *Posidonia Oceanica*, Polymer Degradation and Stability, 121, 105-115" is available at: <https://doi.org/10.1016/j.polyimdegradstab.2015.08.016>

1  
2           **Study of disintegrability in compost and enzymatic degradation of PLA and PLA**  
3           **nanocomposites reinforced with cellulose nanocrystals extracted from *Posidonia Oceanica***

4                           F. Luzi, E. Fortunati\*, D. Puglia, R. Petrucci, J.M. Kenny, L. Torre

5  
6           University of Perugia, Civil and Environmental Engineering Department, UdR INSTM, Strada di  
7                           Pentima 4, 05100 Terni (Italy)

8  
9           \***Corresponding author:** Tel.: +39-0744492921; fax: +39-0744492950; E-mail address:  
10           elena.fortunati@unipg.it (E. Fortunati)

11  
12           **Abstract**

13           Nanocomposite films based on poly(lactic acid) (PLA) reinforced with cellulose nanocrystals  
14           extracted from *Posidonia Oceanica* plant were prepared by solvent casting method containing 1 or  
15           3 % wt of cellulose nanocrystals unmodified (CNC) and modified using a commercial surfactant (s-  
16           CNC). The modification **improves** the dispersion of CNC into the matrix. Enzymatic degradation  
17           using efficient enzyme proteinase K and disintegrability in composting conditions were considered  
18           to gain insights **into the post-use** degradation processes of the produced formulations. Results of  
19           visual, morphological and thermal analysis of enzymatic degradation studies confirmed that the  
20           selected enzyme preferentially degraded amorphous regions with respect of crystalline ones, while  
21           the crystallinity degree of the nanocomposite films increased during enzymatic degradation, as a  
22           consequence of enzyme action. The disintegration in composting conditions of different  
23           formulations was also investigated by means of visual and morphological analysis. The  
24           **disintegrability in compost conditions** showed that the formulations disintegrated in less than 14  
25           days, in addition it has been proved that CNC modified with surfactant were able to promote the  
26           disintegration behaviour. The production of PLA based nanocomposites incorporating cellulose

27 extract from marine wastes suggested the potential application of the proposed material for short-  
28 term food packaging with low environmental impact.

29

30 **Keywords:** poly(lactic acid), cellulose nanocrystals, *Posidonia Oceanica*, nanocomposites,  
31 enzymatic degradation, compost disintegrability.

32

## 2 1. Introduction

3 In the last years, biodegradable polymers, that can be decomposed by fungal or microorganisms,  
4 have been considered as promising alternative to **petrochemical**-based polymers for specific  
5 applications [1].

6 Every year, 140 million tons of petroleum based polymers are produced and introduced in the  
7 ecosystem as industrial waste products [2]. Biodegradable polymers are based on renewable  
8 materials, such as starch, lignin, cellulose etc., or synthesized from renewable resources. The green  
9 materials have a lower negative **environmental** impact than the petroleum based materials. Poly  
10 (lactic acid) (PLA) is one of the most attractive green plastic useful for the production of  
11 ecofriendly food packaging [3], it can be degraded into CO<sub>2</sub> and H<sub>2</sub>O [4]. It is a linear aliphatic  
12 thermoplastic polyester derived from renewable resources such as fermentation of starch and other  
13 polysaccharides [5] like corn, rice and sugar beets [6]. PLA is a biocompatible, biodegradable and  
14 crystalline polymer, **the products manufactured using this matrix completely** disintegrated in less  
15 than one month in ideal conditions or in specific medium or environments [7]. Moreover, PLA can  
16 be processed by injection molding, film extrusion, blow molding, thermoforming, fiber spinning,  
17 and film forming and has better thermal processability in comparison with other biopolymers, such  
18 as poly ( $\epsilon$ -caprolactone)(PCL), poly(hydroxyl alkanates) (PHAs), etc. [8, 9].

19 The properties of PLA are dependent on the ratio of D and L enantiomers [10]. **It exhibits**  
20 interesting physical [1] and functional properties as good transparency, good mechanical properties  
21 and low cost.

22 PLA is approved by the Food and Drug Administration (FDA) and can be used in biomedical  
23 application, in direct contact with biological fluids and for implantation in the human body and does  
24 not produce toxic components [11] or carcinogenic effects in local tissues [8] during the  
25 degradation into the body [12]. However, PLA matrix exhibits some limitations when it is used in  
26 food applications compared to equivalent traditional polymers, as lower barrier properties

1 (important properties for food packaging), high brittleness, slow crystallization rate and relatively  
2 low thermal and mechanical properties [13]. In order to overcome these limitations, several  
3 strategies can be adopted to decrease and modulate these properties. The development of  
4 nanocomposites or blends represents a valid **solution** to modify the initial characteristics. The  
5 production of nanocomposites reinforced with nanofiller extracted from natural resources is a valid  
6 strategy used to increase the physical properties of renewable and biodegradable polymers, without  
7 affecting their transparency properties.

8 Cellulose nanocrystals have received, in the last period, a big interest as natural reinforcement able  
9 to increase the properties of a biomaterial suitable for food packaging applications [14]. Moreover,  
10 CNC present excellent biocompatibility [15], high stiffness and low density [16]. CNC can be  
11 extracted from different natural resources as *Cynara Cardunculus* [17], bamboo [18], phormium,  
12 flax [19] and **other** natural sources and waste [20, 21]. The obtained nanostructures are usually  
13 characterized by rigid rod monocrystalline domains with diameters ranging from 1-100 nm and  
14 from ten to hundreds of nm in length [22]. In general, the nanocrystals aspect ratio  
15 (diameter/length) can vary from 1:1 to 1:100 and the dimensions of the CNC depend on the raw  
16 material utilized for their extraction [23] and the intensity of the chemical process for their  
17 production [24]. CNC have a crystalline structure [25] and an elastic modulus around 150 GPa [26].  
18 In this research, CNC extracted from *Posidonia Oceanica* ball wastes have been used. This aquatic  
19 plant appears on Mediterranean coastal beaches in big amounts in the form of balls as a consequence  
20 of storms that tear off leaves and stems in some cases [27], consequently, the plants have to be  
21 removed to maintain the optimum condition of the coastal for the tourists. Several academic  
22 research have focused their attention on the revalorization of ligno-cellulosic wastes of *Posidonia*  
23 *Oceanica* plant [28-30] as reinforcement or nanoreinforcement in different matrices for bio-based  
24 films [31, 32] or as filler for traditional polymer [27].

25 Recently, Fortunati et al. 2015 [32] reported the preparation of CNC extracted from *Posidonia*  
26 *Oceanica* balls; in the same research, they also presented the production and the characterization of

1 PLA based nanocomposites reinforced with cellulose nanocrystals unmodified (CNC) and modified  
2 (s-CNC) with a surfactant. The use of surfactant is a valid strategy to improve the dispersion of the  
3 CNC in a polymeric matrix [33]. The positive results obtained by functional, optical and migration  
4 properties of PLA based films suggested the possibility of using these bio-based nanocomposites in  
5 industrial application.

6 In the present work, enzymatic degradation and disintegrability in composting conditions of PLA  
7 nanocomposites reinforced with both unmodified and surfactant modified cellulose nanocrystals  
8 extracted from *Posidonia Oceanica* balls have been tested, in order to evaluate the post-use  
9 behaviour of these potential food packaging systems. The disintegrability in compost was carried  
10 out at 58 °C in aerobic condition and 50 % of humidity.

11 The enzyme selected for the enzymatic degradation test, a protease from *Tritirachium album*,  
12 proteinase K, was found to be able to degrade selectively L-lactic bonds and not the D-lactic ones,  
13 being poly(D- lactic) not degradable with this specific enzyme [34, 35]. The enzyme shows the  
14 major effect on degradation in amorphous region respect to crystalline ones [35-37]. In fact as  
15 previously reported in literature the degradation rates of PLA decreased with an increase in  
16 crystallinity [38].

17 Visual observation and morphological analysis were performed at different times for each test, with  
18 the aim of evaluating how the two different procedures influenced the properties of the films.  
19 Moreover, thermal analysis was carried out only for film tested in enzymatic degradation  
20 conditions, in order to highlight how proteinase K selectively degraded amorphous regions with  
21 respect of crystalline ones.

22

## 23 **2.Experimental section**

### 24 **2.1 Materials**

25 Poly(lactic acid) (PLA) in forms of fibres (specific gravity 1.25 g cm<sup>-3</sup>, 6 mm length), was supplied  
26 by MiniFibers, Inc..

1 *Posidonia Oceanica* waste balls were collected from the Campello Beach in Alicante (Spain), by  
2 Aitex (Alcoy, Alicante, Spain). *Posidonia Oceanica* is a Mediterranean endemic alga characterized  
3 by relatively high amounts of extractives. The preparation of the cellulose nanocrystals (CNC)  
4 extracted from *Posidonia Oceanica* was previously described [32]. Briefly, the extraction procedure  
5 of cellulose nanocrystals was implemented in two steps (Figure 1). The first step, a chemical alkali  
6 treatment, leads to the production of holocellulose by the gradual removal of lignin, while the  
7 subsequent sulphuric acid hydrolysis process allows obtaining cellulose nanocrystals in an aqueous  
8 suspension from *Posidonia Oceanica* wastes. The mean diameter of the unbleached fibres was  
9  $84 \pm 26$   $\mu\text{m}$ , however, after bleaching pre-treatments as a consequence of elimination of lignin, the  
10 fibres appeared separated and the mean diameter reduced at about  $7 \pm 2$   $\mu\text{m}$ . The CNC appear  
11 individualized and with acicular rod shape,  $(180 \pm 28)$  nm in length a diameter of  $(4.9 \pm 1.3)$  with a  
12 aspect/ratio of 36.7 [32].

13 Tris(hydroxymethyl)aminomethane/HCl, sodium azide, and proteinase K obtained from  
14 *Tritirachium album* (lyophilized powder,  $\geq 30$  units/mg protein) and all the chemical reagents were  
15 supplied by Sigma Aldrich®.

16

## 17 **2.2 PLA nanocomposite processing**

18 PLA nanocomposite films reinforced with CNC and s-CNC were prepared by solvent casting  
19 method using chloroform. Firstly, PLA (0.75 g) was dissolved in 25 mL of  $\text{CHCl}_3$  with stirring at  
20 room temperature (RT). Then specific amount of cellulose nanocrystals (1 wt% and 3 wt% of  
21 unmodified (CNC) and modified with commercial surfactant(s-CNC)), were added, and related  
22 samples, designed respectively as PLA\_1CNC, PLA\_3CNC, PLA\_1s-CNC and PLA\_3s-CNC,  
23 were produced. The CNC were modified with a commercial surfactant (Beycostat A B09 - CECCA  
24 S.A.) [39], an acid phosphate ester of ethoxylatednonylphenol, with the aim of improving both the  
25 dispersion of the nanoreinforcements into the matrix and the final properties of the nanocomposites.  
26 The solution of s-CNC was prepared adding the surfactant in the proportion of 1/4 (wt/wt) directly

1 to the CNC aqueous solution. In order to increase the thermal stability of the produced nanocrystals,  
2 the pH of CNC and s-CNC aqueous solutions was raised to approximately 9, by using a 0.25 %wt  
3 NaOH solution [40].

4 The CNC in powder (unmodified and modified) was added to the CHCl<sub>3</sub>, forming 1 wt%  
5 suspension. The cellulose nanocrystal solution was exposed to sonication (Vibracell, 750W) for 1  
6 min in an ice bath. The different solutions were cast onto a 15 cm diameter glass Petri dish and then  
7 dried for 24 h at RT.

### 8

### 9 **2.3 Disintegrability in composting of PLA and PLA nanocomposites**

10 Disintegrability in composting conditions was carried out following the European standard ISO  
11 20200. The test method determines, at laboratory-scale, the degree of disintegration of plastic  
12 materials under simulated intensive aerobic composting condition [41]. This method studies the  
13 disintegration and not the biodegradability of plastic materials. The degree of disintegration *D* was  
14 calculated in percent by normalizing the sample weight at different days of incubation to the initial  
15 weight by using Equation (1):

$$16 \quad D = \frac{m_i - m_r}{m_i} * 100 \quad (\text{Eq. 1})$$

17 where:

18 *m<sub>i</sub>* = is the initial dry plastic mass;

19 *m<sub>r</sub>* = is the dry plastic material after the test.

20 PLA and PLA nanocomposite films of dimension 15 mm x 15 mm x 0.03 mm were weighed and  
21 buried into the organic substrate at 4-6 cm depth in the perforated boxes guarantying the aerobic  
22 conditions and incubated at 58 °C at 50 % of humidity. The aerobic conditions were guaranteed by  
23 mixing periodically the solid soil. The materials tested can be considered disintegrable according to  
24 the European standard when 90% of the plastic sample weight shall be lost within 90 days of  
25 analysis. In order to simulate the disintegrability in compost, a solid synthetic waste was prepared,

1 mixing sawdust, rabbit food, compost inoculum supplied by Genesu S.p.a., starch, sugar, oil and  
2 urea. The water content of the substrate was around 50 % and the aerobic condition was guaranteed  
3 into the boxes by hand mixing the materials every day. The different formulations were tested for  
4 maximum 14 days. The samples tested were taken out at different times (1, 3, 7, 10 and 14 days),  
5 washed with distilled water and dried in a oven at 37 °C for 24 h.

6 The photographs on the samples were taken for visual comparison, while the surface microstructure  
7 of the PLA and PLA nanocomposites was investigated, before and after 3 days of incubation, by  
8 means of a field emission scanning electron microscope (FESEMSupra 25-Zeiss), after gold  
9 sputtering of the samples.

10

#### 11 **2.4 Enzymatic degradation of PLA and PLA nanocomposites**

12 For enzymatic degradation analysis, each sample was cut with **dimensions** of 15 x 15 x 0.03 mm,  
13 and weighed before its immersion in the degradation medium. After that, the samples were placed  
14 in vials filled with degradation medium formed by the enzyme (0.5 mg) and 5 mL of  
15 tris(hydroxymethyl)aminomethane/HCl buffer (0.05 M, pH 8.6), to optimize the enzyme activity.  
16 Sodium azide (0.02 wt %) was added to each buffer solution to inhibit the growth of  
17 microorganisms. Enzymatic degradation was performed in an incubator at 37 °C and the buffer-  
18 enzyme system was renewed every 24 hours for 21 days to maintain the enzymatic activity.  
19 Specimens (in triplicate) of each formulation were removed for the different time selected for this  
20 study. The samples tested were taken out at 2, 6, 18 and 24 hours and at 1, 2, 3, 5, 7, 8, 9, 16 and 21  
21 days, washed with distilled water and dried at room temperature up to constant weight.

22 Weight measurements, determined using an analytical balance ( $\pm 0.00001$  g), and visual  
23 observations, were performed for each specimen. The weight loss (WL) of the samples was  
24 evaluated by using by using Equation (2):

$$25 \quad WL(\%) = \frac{(W_0 - W_t)}{W_0} * 100 \quad (\text{Eq. 2})$$

1 where:

2  $W_0$  is the initial dry plastic mass;

3  $W_t$  is the dry weight of a material after enzymatic degradation.

4 Another important parameter to be considered is the water absorption (WA) during the degradation  
5 process, the hydrophilic polymers take up water and the degradation rate increase [42]. It was  
6 calculated by using Equation (3):

$$7 \quad WA(\%) = \frac{(W_w - W_t)}{W_t} * 100 \quad (\text{Eq. 3})$$

8 where:

9  $W_w$  is the weight of plastic material after enzymatic degradation;

10  $W_t$  is the dry weight of a material after enzymatic degradation.

11 Thermal characterization after enzymatic degradation was performed using differential scanning  
12 calorimetry (DSC) and thermogravimetric analysis (TGA) at different incubation times. Differential  
13 scanning calorimeter (DSC, Mettler Toledo 822/e) investigations were done from -25 to 210°C, at  
14 10 °C min<sup>-1</sup>, applying two heating and one cooling scans in nitrogen atmosphere (50mL min<sup>-1</sup>).  
15 Melting and cold crystallization temperatures and enthalpies ( $T_m$ ,  $T_{cc}$  and  $\Delta H_m$ ,  $\Delta H_{cc}$ ) were  
16 determined from the first and second heating scan, while crystallization phenomena were analyzed  
17 during the cooling scan. The glass transition temperature ( $T_g$ ) was registered for each scan. Three  
18 samples were used to characterize each formulation.

19 The crystallinity degree was calculated by using Equation (4):

$$20 \quad \chi = \frac{1}{(1 - m_f)} \left[ \frac{(\Delta H_m - \Delta H_{cc})}{\Delta H_0} \right] * 100 \quad (\text{Eq. 4})$$

21 where  $\Delta H_m$  is the melt enthalpy and  $\Delta H_{cc}$  is the cold crystallization enthalpy,  $\Delta H_0$  is enthalpy of  
22 melting for a 100% crystalline PLA sample, taken as 93 J g<sup>-1</sup> [43],  $m_f$  is the weight fraction of  
23 nanoreinforcements in the sample and  $(1 - m_f)$  is the weight fraction of PLA in the sample.

1 Thermogravimetric analysis (TGA - Seiko Exstar 6300) from 30 to 600 °C at 10 °C min<sup>-1</sup> under a  
2 nitrogen atmosphere (250 mL min<sup>-1</sup>) on 10 mg weight was performed for each sample.  
3 Finally, the surface microstructure of the PLA nanocomposites before and after enzymatic  
4 degradation at different incubation times was investigated by FESEM.

5

## 6 **2.5 Statistical analysis**

7 Statistical analysis of data was performed through analysis of variance (ANOVA) using  
8 Statgraphics Plus for Windows 5.1 Program (Munugistics Corp., Rockville, MD). Fisher's least  
9 significant difference (LSD) was used at the 95% confidence.

10

## 11 **3. Results and Discussion**

### 12 **3.1 Disintegrability in composting conditions of PLA and PLA nanocomposites**

13 The disintegrability in composting conditions of PLA and PLA based nanocomposites represents an  
14 interesting and attractive property for packaging applications that simulate the post-use of plastics  
15 [44, 45]. Composting is a natural process, in which the organic material can be decomposed by  
16 microorganisms, including fungi and bacteria. PLA degradation starts with diffusion of water into  
17 the materials. The hydrolysis of PLA produces a molecular weight reduction by random non-  
18 enzymatic chain scissions of the ester groups, leading to the formation of oligomers and lactic acid.  
19 The disintegrability in composting made by microorganisms such as fungi and bacteria starts when  
20 the molecular weight of PLA reaches about 10.000-20.000 g mol<sup>-1</sup>. The microorganisms metabolize  
21 the macromolecules as organic matter, converting them to carbon dioxide, water and humus [44].  
22 The use of nanoparticles, as nanoreinforcements, influence the biodegradation in compost of PLA  
23 and the disintegrability process strongly depends on their hydrophilicity and their nature [46, 47].

24 Figure 2 shows the visual observation (Figure 2,a) and the disintegrability values (Figure 2,b) of the  
25 PLA samples reinforced with both unmodified and surfactant modified CNC extracted from  
26 *Posidonia Oceanica* taken out at different times of composting. The disintegrability value was

1 evaluated in terms of weight loss as a function of testing time, in which the line at 90 % of  
2 disintegration represents the limit point of disintegrability imposed by the ISO 20200; Figure 2,b  
3 shows that all the materials reach a degree of disintegration exceeding 90% after 14 days of  
4 composting, showing an evident visual fragmentation. After only one day of incubation, the  
5 samples start to change their appearance, as it is possible to see in Figure 2,a: the formulations  
6 appear white and deformed and this effect is more evident after 3 days in composting conditions.  
7 The whitening process and the formulation opacity are attributed to change in the refractive index  
8 due to water absorption, with the formation of low molecular weight compounds [47], the **creation**  
9 **of** some holes on the materials and an induced increase of the crystallinity during degradation [48].  
10 Moreover, after 3 days of incubation, PLA\_3s-CNC film became breakable respect to the other  
11 samples, due to the different morphology of the cross section that characterized this sample, as  
12 reported by Fortunati et al 2015 [32]. The cross section of PLA\_3s-CNC system, in fact, appears  
13 characterized by a porous structure induced by the presence of the surfactant. The presence of the  
14 pores favors the process of disintegrability in composting since the internal structure is easily  
15 accessible by water and microorganisms. After 7 days of incubation, the films became breakable  
16 and the weight loss considerably increases; the PLA\_CNC formulations show a reduction in weight  
17 of 30-40%, while the PLA\_s-CNC based systems show a higher reduction, reaching a 70% of  
18 disintegrability for the film reinforced with 3 %wt of cellulose nanocrystals. This different  
19 behaviour is correlated to the different morphology of cross sections and to the presence of  
20 hydrophilic surfactant in PLA\_s-CNC based nanocomposites. The lower disintegration rate  
21 obtained for PLA\_CNC was attributed to the cellulose nanocrystal introduction that, increasing the  
22 crystallinity of the systems, affects the water diffusion through the PLA matrix and, consequently,  
23 the disintegration kinetics [45]. The addition of hydrophilic cellulose is expected to accelerate the  
24 degradation rate in PLA nanocomposites, but at the same time CNC could also inhibit water  
25 diffusion, thus explaining the obtained results [49].

1 Figure 3 shows the FESEM images of the neat PLA and PLA nanocomposites surfaces before and  
2 after 3 days in composting conditions. After 3 days at 58 °C, a clear surface erosion with the  
3 appearance of holes and porous structures on PLA and all PLA nanocomposites was observed,  
4 particularly visible in the PLA\_3s-CNC samples [50, 51]. Moreover, the disintegrability experiment  
5 took place at 58 °C, temperature higher of the nanocomposite glass transition temperature ( $T_g$ )  
6 (Table 1 time 0). The higher temperature and the surfactant presence are able to increase the chain  
7 mobility [45] facilitating the formation of pores structures on the sample surfaces. The breakable  
8 structure facilitates the polymer erosion by microorganisms attack. The erosion surface after 3 days  
9 was no so evident for the CNC based systems, confirming the potentiality of the cellulose crystals  
10 to induce the crystallization of PLA polymer and to inhibit the diffusion process acting by barrier  
11 agents [52, 53].

### 13 **3.2 Enzymatic degradation of PLA and PLA nanocomposites**

14 Figure 4 shows the images of different films (Figure 4,a,b- Panel A) and weigh loss curves (Figure  
15 4,a-b - Panel B) of the studied samples as a function of different degradation times. After 6 hours of  
16 incubation, the samples start to change, as it is possible to see by visual observation (Figure 4,a); the  
17 transparency clearly decreases and all the formulations appear opaque, white and deformed. After  
18 24 hours in the medium, PLA and PLA nanocomposites show a linear increase of the weight loss. It  
19 was observed a higher degradation for PLA neat films with respect to PLA nanocomposites. After  
20 only 24 hours of incubation, the PLA showed up to  $(88.3 \pm 1.4)$  % of weight loss. These results  
21 confirm that PLA degradation is catalysed by proteinase K [35, 54]. **On the other hand**, PLA and  
22 PLA reinforced with CNC appeared degraded after 6 hours of test reaching 40-60 % of degradation  
23 while PLA reinforced with s-CNC maintained the weight loss lower to 10 % (Figure 4 a, Panel B).  
24 Specifically, the weight loss of neat PLA is  $(88.3 \pm 1.4)$ % after 24 h, followed by PLA\_1CNC  
25  $(69.0 \pm 0.9)$  %, PLA\_3CNC  $(63.2 \pm 3.7)$  %, while the weight loss is  $(16.6 \pm 1.3)$  % and  $(23.1 \pm 2.3)$  %,  
26 for PLA\_1-s-CNC and PLA\_3-s-CNC, respectively.

1 The different behaviour that characterizes the CNC and s-CNC based formulations can be attributed  
2 to the presence of surfactant. In detail, we notice that the surfactant, an acid phosphate ester of  
3 ethoxylatednonyl phenol, is able to decrease the pH level of the aqueous solution (pH = 4-5)  
4 inhibiting the action of the enzyme that needs a pH ranged from 7.5 to 12 to explain its action [35,  
5 41, 55].

6 Figure 5 shows the water absorption during the first 24 hours (Figure 5, a) till to 21 days (Figure 5,  
7 b). All the formulations reach the saturation limit of water absorption after 18 hours in contact with  
8 the enzyme containing solution. The formulations reinforced with s-CNC show higher water  
9 absorption values; this behaviour can be related to the presence of micro-holes, basically due to the  
10 presence of the hydrophilic surfactant used to improve the dispersion of CNC into the matrix, as  
11 previously reported [32].

12 FESEM images of the samples, at different incubation times during enzymatic degradation, are  
13 reported in Figure 6. After 2 hours, a change in the system morphologies was observed. A clear  
14 surface erosion with several and tiny holes and channels on PLA and PLA\_CNC surfaces are  
15 observed. A similar result about morphological investigation was previously obtained by Malwela  
16 et Ray (2015) in the enzymatic degradation study of PLA/PBSA blend composites [55]. The surface  
17 modification and the presence of holes and the porous structures can be due to the degradation of  
18 the amorphous region eroded preferentially by proteinase K [35, 56]. This effect is not so evident in  
19 the case of PLA\_s-CNC based formulations, that maintain their original topography till 24 h of  
20 incubation with the enzyme. A more evident surface erosion for PLA\_s-CNC based formulations is  
21 visible after 3 and 7 days in contact with the enzyme containing solution in accord with the slower  
22 degradation kinetic detected by the weight loss measurements previously discuss.

23

### 24 **3.2.1 Thermal properties of PLA nanocomposites after enzymatic degradation**

25 The thermal properties of PLA and PLA nanocomposites at different incubation times are  
26 investigated by TGA and DSC. The derivative curves of the mass loss (DTG) for the different

1 studied formulations are reported in Figure 7, while the DSC thermal properties are summarized in  
2 Table 1 and Figure 8 (first heating scans for all the materials).

3 Thermogravimetric analysis (Figure 7) of PLA revealed a reduction of the **main peak temperature**  
4 **(temperature of maximum degradation rate)** that shifts of about 20 °C to lower temperature, after  
5 only 2 hours in contact with the enzyme (Figure 7, a). Moreover, the PLA maximum degradation  
6 temperature shifts from 332 °C to 278 °C after 2 days of incubation (2 days represent the last time  
7 for PLA enzymatic degradation). A different behaviour is detected for PLA reinforced with  
8 unmodified and modified cellulose nanocrystals. The main degradation temperature of PLA\_1CNC  
9 and PLA\_3CNC during the enzymatic degradation remains unmodified as previously observed in  
10 literature proving that CNC are able to improve the thermal stability of the PLA matrix (Figure 7,  
11 b,c) [44, 54]. PLA\_1s-CNC and PLA\_3s-CNC curves (Figure 7, d,e) show two main **peaks** of  
12 degradation: the first one is associated to the PLA degradation around 330 °C while the **second one**,  
13 at around 500 °C, is related to the surfactant degradation [40]. The variation of the main  
14 degradation **peaks** becomes relevant when the surfactant starts **to be released** from the formulations  
15 and the evidence of the surfactant release from the s-CNC based films is **clearly** detected in the  
16 insert of Figure 7, e. When the surfactant weight starts to decrease (reduction in the intensity of the  
17 peak at around 500 °C), also the **maximum degradation peak** starts to shift to lower temperature as  
18 evidence of the occurring degradation mechanism. In particular, the weight loss of PLA\_1s-CNC  
19 formulation increases after 8 days in enzymatic medium and the same phenomenon is detected for  
20 PLA\_3s-CNC after 2 days of incubation. As just discussed above, the presence of surfactant in the  
21 PLA nanocomposites improves the dispersion of CNC but at same time obstacles the enzyme  
22 activity modifying **the pH of the medium** [42]. Moreover, a higher **degradation kinetics** of PLA\_3s-  
23 CNC with respect to the PLA\_1s-CNC is observed. The degradation of PLA\_3s-CNC is accelerated  
24 by the presence of several holes on the fractured surface [32] that facilitated the hydrolytic  
25 degradation of the PLA. In particular, the main peak for PLA\_1-s-CNC, shifts from 330 °C to 302  
26 °C after 21 days while PLA\_3-s-CNC reaches 304 °C after only 5 days.

1 Figure 8 shows the DSC thermograms related to the first heating scan, underlining the variation of  
2 crystallization and melting properties at the beginning and at the end of the enzymatic degradation  
3 test. The DSC experiments are performed with the aim of investigating the thermal behaviour of  
4 PLA nanocomposites during the enzymatic degradation. As it is possible to observe, for PLA and  
5 PLA\_CNC systems the peak of the cold crystallization disappears completely at the end of test,  
6 while for PLA\_s-CNC based nanocomposites the peak decreases in its intensity. The melting peak  
7 of nanocomposites at initial time is characterized by the presence of two melting peaks. The first  
8 peak disappears during the degradation test as observed by thermograms and as reported in Table 1.  
9 During the first heating scan (Table 1) some changes are observed in glass transition temperature,  
10 cold crystallization temperature, melting enthalpy and cold crystallization enthalpy while for the  
11 second value of melting temperature not significant changes are detected. The cold crystallization  
12 enthalpy decreases, while the melting enthalpy increases with the time encouraging the  
13 crystallization according with literature [42]. The crystallinity degree values, calculated at time  
14 zero, are  $(8.9\pm3.4)$ ,  $(8.6\pm3.0)$ ,  $(7.5\pm1.7)$ ,  $(9.5\pm0.2)$  and  $(11.4\pm2.0)$  respectively for PLA,  
15 PLA\_1CNC, PLA\_3CNC, PLA\_1s-CNC and PLA\_3s-CNC. The same values, calculated at the  
16 final stage of the enzymatic degradation for each formulations, increased up to  $(35.4\pm0.8)$ ,  
17  $(31.9\pm0.9)$ ,  $(24.5\pm0.7)$ ,  $(35.1\pm3.7)$  and  $(31.1\pm0.5)$  respectively for PLA, PLA\_1CNC, PLA\_3CNC,  
18 PLA\_1s-CNC and PLA\_3s-CNC. The **increase in crystallinity** degree highlights the action of  
19 specific enzyme able to degrade amorphous regions [35]. The **increase in crystallinity** degree can be  
20 correlated to the visual appearance of the sample surfaces of PLA and PLA nanocomposites: the  
21 films change the colour becoming white, opaque and deformed. Moreover, the two melting peaks of  
22 neat PLA, PLA\_1CNC PLA\_3CNC are associated to the coexistence of two kinds of crystalline  
23 structure of PLA [57], while this effect is not evident in the case of PLA reinforced with s-CNC.

24

#### 25 **4. Conclusions**

1 This research involved two different studies for simulation, at laboratory scale, of the post use of  
2 nanocomposite films based on poly(lactic acid) (PLA) and cellulose nanocrystals (CNC) extracted  
3 from *Posidonia Oceanica* plant prepared by solvent casting method. The films disintegrated  
4 completely during 14 days of the test. The disintegration rate in composting condition was  
5 increased by the presence of s-CNC, due to the hydrophilicity of the surfactant. In particular, the  
6 disintegrability of PLA\_3s-CNC is accelerated by the presence of holes detected by morphology  
7 study on cross section surfaces.

8 Proteinase K strongly catalysed the degradation of PLA and PLA nanocomposites, this effect was  
9 delayed in PLA\_s-CNC based nanocomposites. This behaviour can be related to the presence of  
10 surfactant that, in enzymatic buffer, can be released changing the optimum conditions for the  
11 enzyme activity. In fact, it was observed that the degradation values in enzyme buffer for PLA\_s-  
12 CNC increased with decreased presence of surfactant, as detected by thermogravimetric analysis.  
13 PLA and PLA\_CNC films degraded completely in two days in enzymatic medium. Moreover,  
14 proteinase K degraded preferentially the amorphous region with respect of crystalline one. The DSC  
15 analysis confirmed the higher value of crystallinity degrees obtained during the different  
16 degradation times.

17

## 18 **Acknowledgements**

19 The Authors acknowledge the financial support of SEAMATTER: Revalorisation of coastal algae  
20 wastes in textile nonwoven industry with applications in building noise isolation, LIFE11  
21 ENV/E/000600, Funding Program: LIFE+. Call 2011.

22

## 23 **References**

24 1. Stloukal P, Kalendová A, Mattausch H, Laske S, Holzer C, Koutny M. The influence of a  
25 hydrolysis-inhibiting additive on the degradation and biodegradation of PLA and its  
26 nanocomposites. *Polym Test* 2015;41:124-132.

- 1 2. Madhavan Nampoothiri K, Nair NR, John RP. An overview of the recent developments in  
2 polylactide (PLA) research. *Bioresource Technol* 2010;101(22):8493-8501.
- 3 3. Averous L. Biodegradable multiphase systems based on plasticized starch: A review. *J Macromol*  
4 *Sci Polym R* 2004;C44(3):231-274.
- 5 4. Arjmandi R, Hassan A, Eichhorn SJ, Haafiz MKM, Zakaria Z, Tanjung FA. Enhanced ductility  
6 and tensile properties of hybrid montmorillonite/cellulose nanowhiskers reinforced polylactic acid  
7 nanocomposites. *J Mater Sci* 2015;50(8):3118-3130.
- 8 5. Arrieta MP, Samper MD, López J, Jiménez A. Combined Effect of Poly (hydroxybutyrate) and  
9 Plasticizers on Polylactic acid Properties for Film Intended for Food Packaging. *J Polym*  
10 *Environment* 2014;22(2):460-470.
- 11 6. Dong Y, Ghataura A, Takagi H, Haroosh HJ, Nakagaito AN, Lau K-T. Polylactic acid (PLA)  
12 biocomposites reinforced with coir fibres: Evaluation of mechanical performance and  
13 multifunctional properties. *Compos Part A-Appl S* 2014;63:76-84.
- 14 7. Jonoobi M, Harun J, Mathew AP, Oksman K. Mechanical properties of cellulose nanofiber  
15 (CNF) reinforced polylactic acid (PLA) prepared by twin screw extrusion. *Compos Sci Technol*  
16 2010;70(12):1742-1747.
- 17 8. Rasal RM, Janorkar AV, Hirt DE. Poly (lactic acid) modifications. *Prog Polym Sci*  
18 2010;35(3):338-356.
- 19 9. Arrieta MP, López J, Hernández A, Rayón E. Ternary PLA–PHB–Limonene blends intended for  
20 biodegradable food packaging applications. *Eur Polym J* 2014;50(0):255-270.
- 21 10. Abdelwahab MA, Flynn A, Chiou B-S, Imam S, Orts W, Chiellini E. Thermal, mechanical and  
22 morphological characterization of plasticized PLA–PHB blends. *Polym Degrad Stabil*  
23 2012;97(9):1822-1828.
- 24 11. Armentano I, Bitinis N, Fortunati E, Mattioli S, Rescignano N, Verdejo R, Lopez-Manchado  
25 MA, Kenny JM. Multifunctional nanostructured PLA materials for packaging and tissue  
26 engineering. *Progr Polym Sci* 2013;38(10):1720-1747.

- 1 12. Gupta B, Revagade N, Hilborn J. Poly (lactic acid) fiber: an overview. *Progr Polym Sci*  
2 2007;32(4):455-482.
- 3 13. Herrera N, Mathew AP, Oksman K. Plasticized polylactic acid/cellulose nanocomposites  
4 prepared using melt-extrusion and liquid feeding: mechanical, thermal and optical properties.  
5 *Compos Sci Technol* 2015;106:149-155.
- 6 14. Šturcová A, Davies GR, Eichhorn SJ. Elastic Modulus and Stress-Transfer Properties of  
7 Tunicate Cellulose Whiskers. *Biomacromolecules*. 2005;6(2):1055-1061.
- 8 15. Fernandes EM, Pires RA, Mano JF, Reis RL. Bionanocomposites from lignocellulosic  
9 resources: Properties, applications and future trends for their use in the biomedical field. *Progr*  
10 *Polym Sci* 2013;38(10):1415-1441.
- 11 16. Arrieta MP, Fortunati E, Dominici F, Rayón E, López J, Kenny JM. PLA-PHB/cellulose based  
12 films: Mechanical, barrier and disintegration properties. *Polym Degrad Stabil* 2014;107(0):139-149.
- 13 17. Coccia V, Cotana F, Cavalaglio G, Gelosia M, Petrozzi A. Cellulose Nanocrystals Obtained  
14 from *Cynara Cardunculus* and Their Application in the Paper Industry. *Sustainability*  
15 2014;6(8):5252-5264.
- 16 18. Brito BSL, Pereira FV, Putaux J-L, Jean B. Preparation, morphology and structure of cellulose  
17 nanocrystals from bamboo fibers. *Cellulose* 2012;19(5):1527-1536.
- 18 19. Fortunati E, Puglia D, Luzi F, Santulli C, Kenny JM, Torre L. Binary PVA bio-nanocomposites  
19 containing cellulose nanocrystals extracted from different natural sources: Part I. *Carbohydr Polym*  
20 2013;97(2):825-836.
- 21 20. Neto WPF, Silvério HA, Dantas NO, Pasquini D. Extraction and characterization of cellulose  
22 nanocrystals from agro-industrial residue—Soy hulls. *Ind Crop Prod* 2013;42:480-488.
- 23 21 Hsieh Y-L. Cellulose nanocrystals and self-assembled nanostructures from cotton, rice straw and  
24 grape skin: a source perspective. *J Mater Sci* 2013;48(22):7837-7846.

- 1 22. Matos Ruiz M, Cavaillé JY, Dufresne A, Gérard JF, Graillat C. Processing and characterization  
2 of new thermoset nanocomposites based on cellulose whiskers. *Compos Interface* 2000;7(2):117-  
3 131.
- 4 23. Lin N, Dufresne A. Nanocellulose in biomedicine: Current status and future prospect. *Eur*  
5 *Polym J* 2014;59:302-325.
- 6 24. Cranston ED, Gray DG. Morphological and Optical Characterization of Polyelectrolyte  
7 Multilayers Incorporating Nanocrystalline Cellulose. *Biomacromolecules*. 2006;7(9):2522-2530.
- 8 25. Silvério HA, Neto WPF, Dantas NO, Pasquini D. Extraction and characterization of cellulose  
9 nanocrystals from corncob for application as reinforcing agent in nanocomposites. *Ind Crops and*  
10 *Prod* 2013;44:427-436.
- 11 26. Saïd Azizi Samir MA, Alloin F, Paillet M, Dufresne A. Tangling effect in fibrillated cellulose  
12 reinforced nanocomposites. *Macromolecules*. 2004;37(11):4313-4316.
- 13 27. Puglia D, Petrucci R, Fortunati E, Luzi F, Kenny JM, Torre L. Revalorisation of *Posidonia*  
14 *Oceanica* as Reinforcement in Polyethylene/Maleic Anhydride Grafted Polyethylene Composites. *J*  
15 *Renewable Mat* 2014;2(1):66-76.
- 16 28. Bettaieb F, Khiari R, Hassan ML, Belgacem MN, Bras J, Dufresne A, Mhenni MF, Preparation  
17 and characterization of new cellulose nanocrystals from marine biomass *Posidonia oceanica*. *Ind*  
18 *Crop Prod* 2015; doi:10.1016/j.indcrop.2014.12.038.
- 19 29. Bettaieb F, Khiari R, Dufresne A, Mhenni MF, Putaux JL, Boufi S. Nanofibrillar cellulose from  
20 *Posidoniaoceanica*: Properties and morphological features. *Ind Crop Prod* 2015;  
21 doi:10.1016/j.indcrop.2014.12.060
- 22 30. Bettaieb F, Khiari R, Dufresne A, Mhenni MF, Belgacem MN. Mechanical and thermal  
23 properties of *Posidonia oceanica* cellulose nanocrystal reinforced polymer. *Carbohydr Polym*  
24 2015;123:99-104.

- 1 31. Khiari R, Marrakchi Z, Belgacem MN, Mauret E, Mhenni F. New lignocellulosic fibres-  
2 reinforced composite materials: A stepforward in the valorisation of the *Posidonia oceanica* balls.  
3 *Compos Sci Technol* 2011;71(16):1867-1872.
- 4 32. Fortunati E, Luzi F, Puglia D, Petrucci R, Kenny JM, Torre L. Processing of PLA  
5 nanocomposites with cellulose nanocrystals extracted from *Posidonia oceanica* waste: Innovative  
6 reuse of coastal plant. *Ind Crop Prod* 2015;67:439-447.
- 7 33. Petersson L, Kvien I, Oksman K. Structure and thermal properties of poly (lactic acid)/cellulose  
8 whiskers nanocomposite materials. *Compos Sci Technol* 2007;67(11):2535-2544.
- 9 34. Liu L, Li S, Garreau H, Vert M. Selective enzymatic degradations of poly (L-lactide) and poly  
10 ( $\epsilon$ -caprolactone) blend films. *Biomacromolecules*. 2000;1(3):350-359.
- 11 35. Li S, Girard A, Garreau H, Vert M. Enzymatic degradation of polylactide stereocopolymers  
12 with predominant D-lactyl contents. *Polym Degrad Stabil* 2000;71(1):61-67.
- 13 36. Dong J, Liao L, Ma Y, Shi L, Wang G, Fan Z, Li S, Lu Z. Enzyme-catalyzed degradation  
14 behavior of l-lactide/trimethylene carbonate/glycolide terpolymers and their composites with poly  
15 (l-lactide-co-glycolide) fibers. *Polym Degrad Stabil* 2014;103:26-34.
- 16 37. Reeve MS, McCarthy SP, Downey MJ, Gross RA. Polylactide stereochemistry: effect on  
17 enzymic degradability. *Macromolecules* 1994;27(3):825-831.
- 18 38. MacDonald RT, McCarthy SP, Gross RA. Enzymatic degradability of poly (lactide): effects of  
19 chain stereochemistry and material crystallinity. *Macromolecules* 1996;29(23):7356-7361.
- 20 39. Heux L, Chauve G, Bonini C. Nonflocculating and chiral-nematic self-ordering of cellulose  
21 microcrystals suspensions in nonpolar solvents. *Langmuir*. 2000;16(21):8210-8212.
- 22 40. Fortunati E, Armentano I, Zhou Q, Iannoni A, Saino E, Visai L, Berglund LA, Kenny JM.  
23 Multifunctional bionanocomposite films of poly(lactic acid), cellulose nanocrystals and silver  
24 nanoparticles. *Carbohydr Polym* 2012;87(2):1596-1605.
- 25 41. Determination of the degree of disintegration of plastic materials under simulated composting  
26 condition in a laboratory-scale test. UN EN ISO 20200 2006.

- 1 42. Wang C-H, Fan K-R, Hsiue G-H. Enzymatic degradation of PLLA-PEOz-PLLA triblock  
2 copolymers. *Biomaterials* 2005;26(16):2803-2811.
- 3 43. Turner J, Riga A, O'Connor A, Zhang J, Collis J. Characterization of drawn and undrawn poly-  
4 L-lactide films by differential scanning calorimetry. *J Therm Anal Calorim* 2004;75(1):257-268.
- 5 44. Kale G, Kijchavengkul T, Auras R, Rubino M, Selke SE, Singh SP. Compostability of  
6 bioplastic packaging materials: an overview. *Macromol Biosci* 2007;7(3):255-277.
- 7 45. Fortunati E, Luzi F, Puglia D, Dominici F, Santulli C, Kenny JM, Torre L. Investigation of  
8 thermo-mechanical, chemical and degradative properties of PLA-limonene films reinforced with  
9 cellulose nanocrystals extracted from Phormium tenax leaves. *Euro Polym J* 2014;56(0):77-91.
- 10 46. Fukushima K, Abbate C, Tabuani D, Gennari M, Camino G. Biodegradation of poly (lactic  
11 acid) and its nanocomposites. *Polym Degrad Stabil* 2009;94(10):1646-1655.
- 12 47. Bitinis N, Fortunati E, Verdejo R, Bras J, Maria Kenny J, Torre L, López-Manchado MA.  
13 Poly(lactic acid)/natural rubber/cellulose nanocrystal bionanocomposites. Part II: Properties  
14 evaluation. *Carbohydr Polym* 2013;96(2):621-627.
- 15 48. Paul MA, Delcourt C, Alexandre M, Degée P, Monteverde F, Dubois P.  
16 Polylactide/montmorillonite nanocomposites: study of the hydrolytic degradation. *Polym Degrad*  
17 *Stabil* 2005;87(3):535-542.
- 18 49. Fortunati E, Peltzer M, Armentano I, Jimenez A, Kenny JM. Combined effects of cellulose  
19 nanocrystals and silver nanoparticles on the barrier and migration properties of PLA nano-  
20 biocomposites. *J Food Eng* 2013;118(1):117-124.
- 21 50. Arrieta MP, López J, Rayón E, Jiménez A. Disintegrability under composting conditions of  
22 plasticized PLA-PHB blends. *Polym Degrad Stabil* 2014; 108: 307-318.
- 23 51. Arias V, Höglund A, Odelius K, Albertsson AC. Polylactides with “green” plasticizers:  
24 Influence of isomer composition. *J Appl Polym Sci* 2013;130(4):2962-2970.

- 1 52. Khan A, Khan RA, Salmieri S, Le Tien C, Riedl B, Bouchard J, Chauve G, Tan V, Kamal MR,  
2 Lacroix M. Mechanical and barrier properties of nanocrystalline cellulose reinforced chitosan based  
3 nanocomposite films. *Carbohydr Polym* 2012;90(4):1601-1608.
- 4 53. Sanchez-Garcia MD, Lagaron JM. On the use of plant cellulose nanowhiskers to enhance the  
5 barrier properties of polylactic acid. *Cellulose* 2010;17(5):987-1004.
- 6 54. Li S, Tenon M, Garreau H, Braud C, Vert M. Enzymatic degradation of stereocopolymers  
7 derived from L-, DL- and meso-lactides. *Polym Degrad Stabil* 2000;67(1):85-90.
- 8 55. Malwela T, Ray SS. Enzymatic degradation behavior of nanoclay reinforced biodegradable  
9 PLA/PBSA blend composites. *Int J Biol Macromol* 2015;77:131-142.
- 10 56. Yamashita K, Kikkawa Y, Kurokawa K, Doi Y. Enzymatic degradation of poly (L-lactide) film  
11 by proteinase K: quartz crystal microbalance and atomic force microscopy study.  
12 *Biomacromolecules* 2005;6(2):850-857.
- 13 57. Yasuniwa M, Tsubakihara S, Sugimoto Y, Nakafuku C. Thermal analysis of the  
14 double - melting behavior of poly (L - lactic acid). *J Polym Sci Pol Phys* 2004;42(1):25-32.

15

16

## 17 **Figure and Table Captions**

18 **Figure 1:** Scheme of CNC extraction process from *Posidonia Oceanica* plant.

19 **Figure 2:** Visual observation (a) and disintegrability values (b) of PLA and PLA nanocomposites  
20 before and after different days under composting conditions.

21 **Figure 3:** FESEM investigation of PLA and PLA nanocomposites before and after 3 days in  
22 composting conditions.

23 **Figure 4:** Panel A: visual observation (a, b) of PLA and PLA nanocomposites at different times of  
24 enzymatic degradation. Panel B: weight loss at different hours (2, 6, 18 and 24 h) (c) and weight  
25 loss at different days (d) in enzymatic medium of PLA and PLA nanocomposites. (Different letters

1 in the graphs c) indicate significant statistical differences among formulations ( $p < 0.05$ ) after 24  
2 hours of test in enzymatic buffer solution).

3 **Figure 5:** Water absorption at different hours (2, 6, 18 and 24 h) (b), and water absorption at  
4 different days (c) in enzymatic medium of PLA and PLA nanocomposites. (Different letters in the  
5 graphs c) indicate significant statistical differences among formulations ( $p < 0.05$ ) after 24 hours of  
6 test in enzymatic buffer solution).

7 **Figure 6:** FESEM investigation of PLA and PLA nanocomposites after enzymatic degradation.

8 **Figure 7:** Derivative curves of weight loss for PLA and PLA nanocomposites at different  
9 enzymatic degradation times.

10 **Figure 8:** DSC thermograms at the first heating scan for PLA and PLA nanocomposites. The black  
11 curve is relative to initial time while the red/ lower curve is referred to the final time of incubation  
12 in enzymatic solution for each formulation.

13

14 **Table 1:** Thermal properties of PLA and PLA nanocomposites at different time of enzymatic  
15 degradation at the first heating scan.

16

17

1           **Study of disintegrability in compost and enzymatic degradation of PLA and PLA**  
2           **nanocomposites reinforced with cellulose nanocrystals extracted from *Posidonia Oceanica***

3  
4           F. Luzi, E. Fortunati<sup>\*</sup>, D. Puglia, R. Petrucci, J.M. Kenny, L. Torre

5  
6           University of Perugia, Civil and Environmental Engineering Department, UdR INSTM, Strada di  
7           Pentima 4, 05100 Terni (Italy)

8  
9           \***Corresponding author:** Tel.: +39-0744492921; fax: +39-0744492950; E-mail address:  
10          elena.fortunati@unipg.it (E. Fortunati)

11  
12          **Abstract**

13          Nanocomposite films based on poly(lactic acid) (PLA) reinforced with cellulose nanocrystals  
14          extracted from *Posidonia Oceanica* plant were prepared by solvent casting method containing 1 or  
15          3 %wt of cellulose nanocrystals unmodified (CNC) and modified using a commercial surfactant (s-  
16          CNC). The modification improves the dispersion of CNC into the matrix. Enzymatic degradation  
17          using efficient enzyme proteinase K and disintegrability in composting conditions were considered  
18          to gain insights into the post-use degradation processes of the produced formulations. Results of  
19          visual, morphological and thermal analysis of enzymatic degradation studies confirmed that the  
20          selected enzyme preferentially degraded amorphous regions with respect of crystalline ones, while  
21          the crystallinity degree of the nanocomposite films increased during enzymatic degradation, as a  
22          consequence of enzyme action. The disintegration in composting conditions of different  
23          formulations was also investigated by means of visual and morphological analysis. The  
24          disintegrability in compost conditions showed that the formulations disintegrated in less than 14  
25          days, in addition it has been proved that CNC modified with surfactant were able to promote the  
26          disintegration behaviour. The production of PLA based nanocomposites incorporating cellulose  
27          extract from marine wastes suggested the potential application of the proposed material for short-  
28          term food packaging with low environmental impact.

29  
30          **Keywords:** poly(lactic acid), cellulose nanocrystals, *Posidonia Oceanica*, nanocomposites,  
31          enzymatic degradation, compost disintegrability.

1  
2  
3  
4  
5  
6  
7  
8  
9  
10  
11  
12  
13  
14  
15  
16  
17  
18  
19  
20  
21  
22  
23  
24  
25  
26

## 1. Introduction

In the last years, biodegradable polymers, that can be decomposed by fungal or microorganisms, have been considered as promising alternative to petrochemical-based polymers for specific applications [1].

Every year, 140 million tons of petroleum based polymers are produced and introduced in the ecosystem as industrial waste products [2]. Biodegradable polymers are based on renewable materials, such as starch, lignin, cellulose etc., or synthesized from renewable resources. The green materials have a lower negative environmental impact than the petroleum based materials. Poly (lactic acid) (PLA) is one of the most attractive green plastic useful for the production of ecofriendly food packaging [3], it can be degraded into CO<sub>2</sub> and H<sub>2</sub>O [4]. It is a linear aliphatic thermoplastic polyester derived from renewable resources such as fermentation of starch and other polysaccharides [5] like corn, rice and sugar beets [6]. PLA is a biocompatible, biodegradable and crystalline polymer, the products manufactured using this matrix completely disintegrated in less than one month in ideal conditions or in specific medium or environments [7]. Moreover, PLA can be processed by injection molding, film extrusion, blow molding, thermoforming, fiber spinning, and film forming and has better thermal processability in comparison with other biopolymers, such as poly (ε-caprolactone)(PCL), poly(hydroxyl alkanates) (PHAs), etc. [8, 9].

The properties of PLA are dependent on the ratio of D and L enantiomers [10]. It exhibits interesting physical [1] and functional properties as good transparency, good mechanical properties and low cost.

PLA is approved by the Food and Drug Administration (FDA) and can be used in biomedical application, in direct contact with biological fluids and for implantation in the human body and does not produce toxic components [11] or carcinogenic effects in local tissues [8] during the degradation into the body [12]. However, PLA matrix exhibits some limitations when it is used in food applications compared to equivalent traditional polymers, as lower barrier properties

1 (important properties for food packaging), high brittleness, slow crystallization rate and relatively  
2 low thermal and mechanical properties [13]. In order to overcome these limitations, several  
3 strategies can be adopted to decrease and modulate these properties. The development of  
4 nanocomposites or blends represents a valid solution to modify the initial characteristics. The  
5 production of nanocomposites reinforced with nanofiller extracted from natural resources is a valid  
6 strategy used to increase the physical properties of renewable and biodegradable polymers, without  
7 affecting their transparency properties.

8 Cellulose nanocrystals have received, in the last period, a big interest as natural reinforcement able  
9 to increase the properties of a biomaterial suitable for food packaging applications [14]. Moreover,  
10 CNC present excellent biocompatibility [15], high stiffness and low density [16]. CNC can be  
11 extracted from different natural resources as *Cynara Cardunculus* [17], bamboo [18], phormium,  
12 flax [19] and other natural sources and waste [20, 21]. The obtained nanostructures are usually  
13 characterized by rigid rod monocrystalline domains with diameters ranging from 1-100 nm and  
14 from ten to hundreds of nm in length [22]. In general, the nanocrystals aspect ratio  
15 (diameter/length) can vary from 1:1 to 1:100 and the dimensions of the CNC depend on the raw  
16 material utilized for their extraction [23] and the intensity of the chemical process for their  
17 production [24]. CNC have a crystalline structure [25] and an elastic modulus around 150 GPa [26].  
18 In this research, CNC extracted from *Posidonia Oceanica* ball wastes have been used. This aquatic  
19 plant appears on Mediterranean coastal beaches in big amounts in the form of balls as a consequence  
20 of storms that tear off leaves and stems in some cases [27], consequently, the plants have to be  
21 removed to maintain the optimum condition of the coastal for the tourists. Several academic  
22 research have focused their attention on the revalorization of ligno-cellulosic wastes of *Posidonia*  
23 *Oceanica* plant [28-30] as reinforcement or nanoreinforcement in different matrices for bio-based  
24 films [31, 32] or as filler for traditional polymer [27].

25 Recently, Fortunati et al. 2015 [32] reported the preparation of CNC extracted from *Posidonia*  
26 *Oceanica* balls; in the same research, they also presented the production and the characterization of

1 PLA based nanocomposites reinforced with cellulose nanocrystals unmodified (CNC) and modified  
2 (s-CNC) with a surfactant. The use of surfactant is a valid strategy to improve the dispersion of the  
3 CNC in a polymeric matrix [33]. The positive results obtained by functional, optical and migration  
4 properties of PLA based films suggested the possibility of using these bio-based nanocomposites in  
5 industrial application.

6 In the present work, enzymatic degradation and disintegrability in composting conditions of PLA  
7 nanocomposites reinforced with both unmodified and surfactant modified cellulose nanocrystals  
8 extracted from *Posidonia Oceanica* balls have been tested, in order to evaluate the post-use  
9 behaviour of these potential food packaging systems. The disintegrability in compost was carried  
10 out at 58 °C in aerobic condition and 50 % of humidity.

11 The enzyme selected for the enzymatic degradation test, a protease from *Tritirachium album*,  
12 proteinase K, was found to be able to degrade selectively L-lactic bonds and not the D-lactic ones,  
13 being poly(D- lactic) not degradable with this specific enzyme [34, 35]. The enzyme shows the  
14 major effect on degradation in amorphous region respect to crystalline ones [35-37]. In fact as  
15 previously reported in literature the degradation rates of PLA decreased with an increase in  
16 crystallinity [38].

17 Visual observation and morphological analysis were performed at different times for each test, with  
18 the aim of evaluating how the two different procedures influenced the properties of the films.  
19 Moreover, thermal analysis was carried out only for film tested in enzymatic degradation  
20 conditions, in order to highlight how proteinase K selectively degraded amorphous regions with  
21 respect of crystalline ones.

22

## 23 **2.Experimental section**

### 24 **2.1 Materials**

25 Poly(lactic acid) (PLA) in forms of fibres (specific gravity  $1.25 \text{ g cm}^{-3}$ , 6 mm length), was supplied  
26 by MiniFibers, Inc..

1 *Posidonia Oceanica* waste balls were collected from the Campello Beach in Alicante (Spain), by  
2 Aitex (Alcoy, Alicante, Spain). *Posidonia Oceanica* is a Mediterranean endemic alga characterized  
3 by relatively high amounts of extractives. The preparation of the cellulose nanocrystals (CNC)  
4 extracted from *Posidonia Oceanica* was previously described [32]. Briefly, the extraction procedure  
5 of cellulose nanocrystals was implemented in two steps (Figure 1). The first step, a chemical alkali  
6 treatment, leads to the production of holocellulose by the gradual removal of lignin, while the  
7 subsequent sulphuric acid hydrolysis process allows obtaining cellulose nanocrystals in an aqueous  
8 suspension from *Posidonia Oceanica* wastes. The mean diameter of the unbleached fibres was  
9  $84 \pm 26$   $\mu\text{m}$ , however, after bleaching pre-treatments as a consequence of elimination of lignin, the  
10 fibres appeared separated and the mean diameter reduced at about  $7 \pm 2$   $\mu\text{m}$ . The CNC appear  
11 individualized and with acicular rod shape,  $(180 \pm 28)$  nm in length a diameter of  $(4.9 \pm 1.3)$  with a  
12 aspect/ratio of 36.7 [32].

13 Tris(hydroxymethyl)aminomethane/HCl, sodium azide, and proteinase K obtained from  
14 *Tritirachium album* (lyophilized powder,  $\geq 30$  units/mg protein) and all the chemical reagents were  
15 supplied by Sigma Aldrich<sup>®</sup>.

16

## 17 **2.2 PLA nanocomposite processing**

18 PLA nanocomposite films reinforced with CNC and s-CNC were prepared by solvent casting  
19 method using chloroform. Firstly, PLA (0.75 g) was dissolved in 25 mL of  $\text{CHCl}_3$  with stirring at  
20 room temperature (RT). Then specific amount of cellulose nanocrystals (1 wt% and 3 wt% of  
21 unmodified (CNC) and modified with commercial surfactant(s-CNC)), were added, and related  
22 samples, designed respectively as PLA\_1CNC, PLA\_3CNC, PLA\_1s-CNC and PLA\_3s-CNC,  
23 were produced. The CNC were modified with a commercial surfactant (Beycostat A B09 - CECCA  
24 S.A.) [39], an acid phosphate ester of ethoxylatednonylphenol, with the aim of improving both the  
25 dispersion of the nanoreinforcements into the matrix and the final properties of the nanocomposites.  
26 The solution of s-CNC was prepared adding the surfactant in the proportion of 1/4 (wt/wt) directly

1 to the CNC aqueous solution. In order to increase the thermal stability of the produced nanocrystals,  
2 the pH of CNC and s-CNC aqueous solutions was raised to approximately 9, by using a 0.25 %wt  
3 NaOH solution [40].

4 The CNC in powder (unmodified and modified) was added to the CHCl<sub>3</sub>, forming 1 wt%  
5 suspension. The cellulose nanocrystal solution was exposed to sonication (Vibracell, 750W) for 1  
6 min in an ice bath. The different solutions were cast onto a 15 cm diameter glass Petri dish and then  
7 dried for 24 h at RT.

### 8

### 9 **2.3 Disintegrability in composting of PLA and PLA nanocomposites**

10 Disintegrability in composting conditions was carried out following the European standard ISO  
11 20200. The test method determines, at laboratory-scale, the degree of disintegration of plastic  
12 materials under simulated intensive aerobic composting condition [41]. This method studies the  
13 disintegration and not the biodegradability of plastic materials. The degree of disintegration  $D$  was  
14 calculated in percent by normalizing the sample weight at different days of incubation to the initial  
15 weight by using Equation (1):

$$16 \quad D = \frac{m_i - m_r}{m_i} * 100 \quad (\text{Eq. 1})$$

17 where:

18  $m_i$  = is the initial dry plastic mass;

19  $m_r$  = is the dry plastic material after the test.

20 PLA and PLA nanocomposite films of dimension 15 mm x 15 mm x 0.03 mm were weighed and  
21 buried into the organic substrate at 4-6 cm depth in the perforated boxes guarantying the aerobic  
22 conditions and incubated at 58 °C at 50 % of humidity. The aerobic conditions were guaranteed by  
23 mixing periodically the solid soil. The materials tested can be considered disintegrable according to  
24 the European standard when 90% of the plastic sample weight shall be lost within 90 days of  
25 analysis. In order to simulate the disintegrability in compost, a solid synthetic waste was prepared,

1 mixing sawdust, rabbit food, compost inoculum supplied by Genesu S.p.a., starch, sugar, oil and  
2 urea. The water content of the substrate was around 50 % and the aerobic condition was guaranteed  
3 into the boxes by hand mixing the materials every day. The different formulations were tested for  
4 maximum 14 days. The samples tested were taken out at different times (1, 3, 7, 10 and 14 days),  
5 washed with distilled water and dried in a oven at 37 °C for 24 h.

6 The photographs on the samples were taken for visual comparison, while the surface microstructure  
7 of the PLA and PLA nanocomposites was investigated, before and after 3 days of incubation, by  
8 means of a field emission scanning electron microscope (FESEMSupra 25-Zeiss), after gold  
9 sputtering of the samples.

10

#### 11 **2.4 Enzymatic degradation of PLA and PLA nanocomposites**

12 For enzymatic degradation analysis, each sample was cut with dimensions of 15 x 15 x 0.03 mm,  
13 and weighed before its immersion in the degradation medium. After that, the samples were placed  
14 in vials filled with degradation medium formed by the enzyme (0.5 mg) and 5 mL of  
15 tris(hydroxymethyl)aminomethane/HCl buffer (0.05 M, pH 8.6), to optimize the enzyme activity.  
16 Sodium azide (0.02 wt %) was added to each buffer solution to inhibit the growth of  
17 microorganisms. Enzymatic degradation was performed in an incubator at 37 °C and the buffer-  
18 enzyme system was renewed every 24 hours for 21 days to maintain the enzymatic activity.  
19 Specimens (in triplicate) of each formulation were removed for the different time selected for this  
20 study. The samples tested were taken out at 2, 6, 18 and 24 hours and at 1, 2, 3, 5, 7, 8, 9, 16 and 21  
21 days, washed with distilled water and dried at room temperature up to constant weight.

22 Weight measurements, determined using an analytical balance ( $\pm 0.00001$  g), and visual  
23 observations, were performed for each specimen. The weight loss (WL) of the samples was  
24 evaluated by using by using Equation (2):

$$25 \quad WL(\%) = \frac{(W_0 - W_t)}{W_0} * 100 \quad (\text{Eq. 2})$$

1 where:

2  $W_0$  is the initial dry plastic mass;

3  $W_t$  is the dry weight of a material after enzymatic degradation.

4 Another important parameter to be considered is the water absorption (WA) during the degradation  
5 process, the hydrophilic polymers take up water and the degradation rate increase [42]. It was  
6 calculated by using Equation (3):

$$7 \quad WA(\%) = \frac{(W_w - W_t)}{W_t} * 100 \quad (\text{Eq. 3})$$

8 where:

9  $W_w$  is the weight of plastic material after enzymatic degradation;

10  $W_t$  is the dry weight of a material after enzymatic degradation.

11 Thermal characterization after enzymatic degradation was performed using differential scanning  
12 calorimetry (DSC) and thermogravimetric analysis (TGA) at different incubation times. Differential  
13 scanning calorimeter (DSC, Mettler Toledo 822/e) investigations were done from -25 to 210°C, at  
14 10 °C min<sup>-1</sup>, applying two heating and one cooling scans in nitrogen atmosphere (50mL min<sup>-1</sup>).  
15 Melting and cold crystallization temperatures and enthalpies ( $T_m$ ,  $T_{cc}$  and  $\Delta H_m$ ,  $\Delta H_{cc}$ ) were  
16 determined from the first and second heating scan, while crystallization phenomena were analyzed  
17 during the cooling scan. The glass transition temperature ( $T_g$ ) was registered for each scan. Three  
18 samples were used to characterize each formulation.

19 The crystallinity degree was calculated by using Equation (4):

$$20 \quad \chi = \frac{1}{(1 - m_f)} \left[ \frac{(\Delta H_m - \Delta H_{cc})}{\Delta H_0} \right] * 100 \quad (\text{Eq. 4})$$

21 where  $\Delta H_m$  is the melt enthalpy and  $\Delta H_{cc}$  is the cold crystallization enthalpy,  $\Delta H_0$  is enthalpy of  
22 melting for a 100% crystalline PLA sample, taken as 93 J g<sup>-1</sup> [43],  $m_f$  is the weight fraction of  
23 nanoreinforcements in the sample and  $(1 - m_f)$  is the weight fraction of PLA in the sample.

1 Thermogravimetric analysis (TGA - Seiko Exstar 6300) from 30 to 600 °C at 10 °C min<sup>-1</sup> under a  
2 nitrogen atmosphere (250 mL min<sup>-1</sup>) on 10 mg weight was performed for each sample.  
3 Finally, the surface microstructure of the PLA nanocomposites before and after enzymatic  
4 degradation at different incubation times was investigated by FESEM.

5

## 6 **2.5 Statistical analysis**

7 Statistical analysis of data was performed through analysis of variance (ANOVA) using  
8 Statgraphics Plus for Windows 5.1 Program (Munugistics Corp., Rockville, MD). Fisher's least  
9 significant difference (LSD) was used at the 95% confidence.

10

## 11 **3. Results and Discussion**

### 12 **3.1 Disintegrability in composting conditions of PLA and PLA nanocomposites**

13 The disintegrability in composting conditions of PLA and PLA based nanocomposites represents an  
14 interesting and attractive property for packaging applications that simulate the post-use of plastics  
15 [44, 45]. Composting is a natural process, in which the organic material can be decomposed by  
16 microorganisms, including fungi and bacteria. PLA degradation starts with diffusion of water into  
17 the materials. The hydrolysis of PLA produces a molecular weight reduction by random non-  
18 enzymatic chain scissions of the ester groups, leading to the formation of oligomers and lactic acid.  
19 The disintegrability in composting made by microorganisms such as fungi and bacteria starts when  
20 the molecular weight of PLA reaches about 10.000-20.000 g mol<sup>-1</sup>. The microorganisms metabolize  
21 the macromolecules as organic matter, converting them to carbon dioxide, water and humus [44].  
22 The use of nanoparticles, as nanoreinforcements, influence the biodegradation in compost of PLA  
23 and the disintegrability process strongly depends on their hydrophilicity and their nature [46, 47].

24 Figure 2 shows the visual observation (Figure 2,a) and the disintegrability values (Figure 2,b) of the  
25 PLA samples reinforced with both unmodified and surfactant modified CNC extracted from  
26 *Posidonia Oceanica* taken out at different times of composting. The disintegrability value was

1 evaluated in terms of weight loss as a function of testing time, in which the line at 90 % of  
2 disintegration represents the limit point of disintegrability imposed by the ISO 20200; Figure 2,b  
3 shows that all the materials reach a degree of disintegration exceeding 90% after 14 days of  
4 composting, showing an evident visual fragmentation. After only one day of incubation, the  
5 samples start to change their appearance, as it is possible to see in Figure 2,a: the formulations  
6 appear white and deformed and this effect is more evident after 3 days in composting conditions.  
7 The whitening process and the formulation opacity are attributed to change in the refractive index  
8 due to water absorption, with the formation of low molecular weight compounds [47], the creation  
9 of some holes on the materials and an induced increase of the crystallinity during degradation [48].  
10 Moreover, after 3 days of incubation, PLA\_3s-CNC film became breakable respect to the other  
11 samples, due to the different morphology of the cross section that characterized this sample, as  
12 reported by Fortunati et al 2015 [32]. The cross section of PLA\_3s-CNC system, in fact, appears  
13 characterized by a porous structure induced by the presence of the surfactant. The presence of the  
14 pores favors the process of disintegrability in composting since the internal structure is easily  
15 accessible by water and microorganisms. After 7 days of incubation, the films became breakable  
16 and the weight loss considerably increases; the PLA\_CNC formulations show a reduction in weight  
17 of 30-40%, while the PLA\_s-CNC based systems show a higher reduction, reaching a 70% of  
18 disintegrability for the film reinforced with 3 %wt of cellulose nanocrystals. This different  
19 behaviour is correlated to the different morphology of cross sections and to the presence of  
20 hydrophilic surfactant in PLA\_s-CNC based nanocomposites. The lower disintegration rate  
21 obtained for PLA\_CNC was attributed to the cellulose nanocrystal introduction that, increasing the  
22 crystallinity of the systems, affects the water diffusion through the PLA matrix and, consequently,  
23 the disintegration kinetics [45]. The addition of hydrophilic cellulose is expected to accelerate the  
24 degradation rate in PLA nanocomposites, but at the same time CNC could also inhibit water  
25 diffusion, thus explaining the obtained results [49].

1 Figure 3 shows the FESEM images of the neat PLA and PLA nanocomposites surfaces before and  
2 after 3 days in composting conditions. After 3 days at 58 °C, a clear surface erosion with the  
3 appearance of holes and porous structures on PLA and all PLA nanocomposites was observed,  
4 particularly visible in the PLA\_3s-CNC samples [50, 51]. Moreover, the disintegrability experiment  
5 took place at 58 °C, temperature higher of the nanocomposite glass transition temperature ( $T_g$ )  
6 (Table 1 time 0). The higher temperature and the surfactant presence are able to increase the chain  
7 mobility [45] facilitating the formation of pores structures on the sample surfaces. The breakable  
8 structure facilitates the polymer erosion by microorganisms attack. The erosion surface after 3 days  
9 was no so evident for the CNC based systems, confirming the potentiality of the cellulose crystals  
10 to induce the crystallization of PLA polymer and to inhibit the diffusion process acting by barrier  
11 agents [52, 53].

12

### 13 **3.2 Enzymatic degradation of PLA and PLA nanocomposites**

14 Figure 4 shows the images of different films (Figure 4,a,b- Panel A) and weigh loss curves (Figure  
15 4,a-b - Panel B) of the studied samples as a function of different degradation times. After 6 hours of  
16 incubation, the samples start to change, as it is possible to see by visual observation (Figure 4,a); the  
17 transparency clearly decreases and all the formulations appear opaque, white and deformed. After  
18 24 hours in the medium, PLA and PLA nanocomposites show a linear increase of the weight loss. It  
19 was observed a higher degradation for PLA neat films with respect to PLA nanocomposites. After  
20 only 24 hours of incubation, the PLA showed up to  $(88.3 \pm 1.4)$  % of weight loss. These results  
21 confirm that PLA degradation is catalysed by proteinase K [35, 54]. On the other hand, PLA and  
22 PLA reinforced with CNC appeared degraded after 6 hours of test reaching 40-60 % of degradation  
23 while PLA reinforced with s-CNC maintained the weight loss lower to 10 % (Figure 4 a, Panel B).  
24 Specifically, the weight loss of neat PLA is  $(88.3 \pm 1.4)$ % after 24 h, followed by PLA\_1CNC  
25  $(69.0 \pm 0.9)$  %, PLA\_3CNC  $(63.2 \pm 3.7)$  %, while the weight loss is  $(16.6 \pm 1.3)$  % and  $(23.1 \pm 2.3)$  %,  
26 for PLA\_1-s-CNC and PLA\_3-s-CNC, respectively.

1 The different behaviour that characterizes the CNC and s-CNC based formulations can be attributed  
2 to the presence of surfactant. In detail, we notice that the surfactant, an acid phosphate ester of  
3 ethoxylatednonyl phenol, is able to decrease the pH level of the aqueous solution (pH = 4-5)  
4 inhibiting the action of the enzyme that needs a pH ranged from 7.5 to 12 to explain its action [35,  
5 41, 55].

6 Figure 5 shows the water absorption during the first 24 hours (Figure 5, a) till to 21 days (Figure 5,  
7 b). All the formulations reach the saturation limit of water absorption after 18 hours in contact with  
8 the enzyme containing solution. The formulations reinforced with s-CNC show higher water  
9 absorption values; this behaviour can be related to the presence of micro-holes, basically due to the  
10 presence of the hydrophilic surfactant used to improve the dispersion of CNC into the matrix, as  
11 previously reported [32].

12 FESEM images of the samples, at different incubation times during enzymatic degradation, are  
13 reported in Figure 6. After 2 hours, a change in the system morphologies was observed. A clear  
14 surface erosion with several and tiny holes and channels on PLA and PLA\_CNC surfaces are  
15 observed. A similar result about morphological investigation was previously obtained by Malwela  
16 et Ray (2015) in the enzymatic degradation study of PLA/PBSA blend composites [55]. The surface  
17 modification and the presence of holes and the porous structures can be due to the degradation of  
18 the amorphous region eroded preferentially by proteinase K [35, 56]. This effect is not so evident in  
19 the case of PLA\_s-CNC based formulations, that maintain their original topography till 24 h of  
20 incubation with the enzyme. A more evident surface erosion for PLA\_s-CNC based formulations is  
21 visible after 3 and 7 days in contact with the enzyme containing solution in accord with the slower  
22 degradation kinetic detected by the weight loss measurements previously discuss.

23

### 24 **3.2.1 Thermal properties of PLA nanocomposites after enzymatic degradation**

25 The thermal properties of PLA and PLA nanocomposites at different incubation times are  
26 investigated by TGA and DSC. The derivative curves of the mass loss (DTG) for the different

1 studied formulations are reported in Figure 7, while the DSC thermal properties are summarized in  
2 Table 1 and Figure 8 (first heating scans for all the materials).

3 Thermogravimetric analysis (Figure 7) of PLA revealed a reduction of the main peak temperature  
4 (temperature of maximum degradation rate) that shifts of about 20 °C to lower temperature, after  
5 only 2 hours in contact with the enzyme (Figure 7, a). Moreover, the PLA maximum degradation  
6 temperature shifts from 332 °C to 278 °C after 2 days of incubation (2 days represent the last time  
7 for PLA enzymatic degradation). A different behaviour is detected for PLA reinforced with  
8 unmodified and modified cellulose nanocrystals. The main degradation temperature of PLA\_1CNC  
9 and PLA\_3CNC during the enzymatic degradation remains unmodified as previously observed in  
10 literature proving that CNC are able to improve the thermal stability of the PLA matrix (Figure 7,  
11 b,c) [44, 54]. PLA\_1s-CNC and PLA\_3s-CNC curves (Figure 7, d,e) show two main peaks of  
12 degradation: the first one is associated to the PLA degradation around 330 °C while the second one,  
13 at around 500 °C, is related to the surfactant degradation [40]. The variation of the main  
14 degradation peaks becomes relevant when the surfactant starts to be released from the formulations  
15 and the evidence of the surfactant release from the s-CNC based films is clearly detected in the  
16 insert of Figure 7, e. When the surfactant weight starts to decrease (reduction in the intensity of the  
17 peak at around 500 °C), also the maximum degradation peak starts to shift to lower temperature as  
18 evidence of the occurring degradation mechanism. In particular, the weight loss of PLA\_1s-CNC  
19 formulation increases after 8 days in enzymatic medium and the same phenomenon is detected for  
20 PLA\_3s-CNC after 2 days of incubation. As just discussed above, the presence of surfactant in the  
21 PLA nanocomposites improves the dispersion of CNC but at same time obstacles the enzyme  
22 activity modifying the pH of the medium [42]. Moreover, a higher degradation kinetics of PLA\_3s-  
23 CNC with respect to the PLA\_1s-CNC is observed. The degradation of PLA\_3s-CNC is accelerated  
24 by the presence of several holes on the fractured surface [32] that facilitated the hydrolytic  
25 degradation of the PLA. In particular, the main peak for PLA\_1-s-CNC, shifts from 330 °C to 302  
26 °C after 21 days while PLA\_3-s-CNC reaches 304 °C after only 5 days.

1 Figure 8 shows the DSC thermograms related to the first heating scan, underlining the variation of  
2 crystallization and melting properties at the beginning and at the end of the enzymatic degradation  
3 test. The DSC experiments are performed with the aim of investigating the thermal behaviour of  
4 PLA nanocomposites during the enzymatic degradation. As it is possible to observe, for PLA and  
5 PLA\_CNC systems the peak of the cold crystallization disappears completely at the end of test,  
6 while for PLA\_s-CNC based nanocomposites the peak decreases in its intensity. The melting peak  
7 of nanocomposites at initial time is characterized by the presence of two melting peaks. The first  
8 peak disappears during the degradation test as observed by thermograms and as reported in Table 1.  
9 During the first heating scan (Table 1) some changes are observed in glass transition temperature,  
10 cold crystallization temperature, melting enthalpy and cold crystallization enthalpy while for the  
11 second value of melting temperature not significant changes are detected. The cold crystallization  
12 enthalpy decreases, while the melting enthalpy increases with the time encouraging the  
13 crystallization according with literature [42]. The crystallinity degree values, calculated at time  
14 zero, are  $(8.9\pm3.4)$ ,  $(8.6\pm3.0)$ ,  $(7.5\pm1.7)$ ,  $(9.5\pm0.2)$  and  $(11.4\pm2.0)$  respectively for PLA,  
15 PLA\_1CNC, PLA\_3CNC, PLA\_1s-CNC and PLA\_3s-CNC. The same values, calculated at the  
16 final stage of the enzymatic degradation for each formulations, increased up to  $(35.4\pm0.8)$ ,  
17  $(31.9\pm0.9)$ ,  $(24.5\pm0.7)$ ,  $(35.1\pm3.7)$  and  $(31.1\pm0.5)$  respectively for PLA, PLA\_1CNC, PLA\_3CNC,  
18 PLA\_1s-CNC and PLA\_3s-CNC. The increase in crystallinity degree highlights the action of  
19 specific enzyme able to degrade amorphous regions [35]. The increase in crystallinity degree can be  
20 correlated to the visual appearance of the sample surfaces of PLA and PLA nanocomposites: the  
21 films change the colour becoming white, opaque and deformed. Moreover, the two melting peaks of  
22 neat PLA, PLA\_1CNC PLA\_3CNC are associated to the coexistence of two kinds of crystalline  
23 structure of PLA [57], while this effect is not evident in the case of PLA reinforced with s-CNC.

24

#### 25 **4. Conclusions**

1 This research involved two different studies for simulation, at laboratory scale, of the post use of  
2 nanocomposite films based on poly(lactic acid) (PLA) and cellulose nanocrystals (CNC) extracted  
3 from *Posidonia Oceanica* plant prepared by solvent casting method. The films disintegrated  
4 completely during 14 days of the test. The disintegration rate in composting condition was  
5 increased by the presence of s-CNC, due to the hydrophilicity of the surfactant. In particular, the  
6 disintegrability of PLA<sub>3</sub>s-CNC is accelerated by the presence of holes detected by morphology  
7 study on cross section surfaces.

8 Proteinase K strongly catalysed the degradation of PLA and PLA nanocomposites, this effect was  
9 delayed in PLA<sub>s</sub>-CNC based nanocomposites. This behaviour can be related to the presence of  
10 surfactant that, in enzymatic buffer, can be released changing the optimum conditions for the  
11 enzyme activity. In fact, it was observed that the degradation values in enzyme buffer for PLA<sub>s</sub>-  
12 CNC increased with decreased presence of surfactant, as detected by thermogravimetric analysis.  
13 PLA and PLA<sub>CNC</sub> films degraded completely in two days in enzymatic medium. Moreover,  
14 proteinase K degraded preferentially the amorphous region with respect of crystalline one. The DSC  
15 analysis confirmed the higher value of crystallinity degrees obtained during the different  
16 degradation times.

17

## 18 **Acknowledgements**

19 The Authors acknowledge the financial support of SEAMATTER: Revalorisation of coastal algae  
20 wastes in textile nonwoven industry with applications in building noise isolation, LIFE11  
21 ENV/E/000600, Funding Program: LIFE+. Call 2011.

22

## 23 **References**

24 1. Stloukal P, Kalendová A, Mattausch H, Laske S, Holzer C, Koutny M. The influence of a  
25 hydrolysis-inhibiting additive on the degradation and biodegradation of PLA and its  
26 nanocomposites. *Polym Test* 2015;41:124-132.

- 1 2. Madhavan Nampoothiri K, Nair NR, John RP. An overview of the recent developments in  
2 polylactide (PLA) research. *Bioresource Technol* 2010;101(22):8493-8501.
- 3 3. Averous L. Biodegradable multiphase systems based on plasticized starch: A review. *J Macromol*  
4 *Sci Polym R* 2004;C44(3):231-274.
- 5 4. Arjmandi R, Hassan A, Eichhorn SJ, Haafiz MKM, Zakaria Z, Tanjung FA. Enhanced ductility  
6 and tensile properties of hybrid montmorillonite/cellulose nanowhiskers reinforced polylactic acid  
7 nanocomposites. *J Mater Sci* 2015;50(8):3118-3130.
- 8 5. Arrieta MP, Samper MD, López J, Jiménez A. Combined Effect of Poly (hydroxybutyrate) and  
9 Plasticizers on Polylactic acid Properties for Film Intended for Food Packaging. *J Polym*  
10 *Environment* 2014;22(2):460-470.
- 11 6. Dong Y, Ghataura A, Takagi H, Haroosh HJ, Nakagaito AN, Lau K-T. Polylactic acid (PLA)  
12 biocomposites reinforced with coir fibres: Evaluation of mechanical performance and  
13 multifunctional properties. *Compos Part A-Appl S* 2014;63:76-84.
- 14 7. Jonoobi M, Harun J, Mathew AP, Oksman K. Mechanical properties of cellulose nanofiber  
15 (CNF) reinforced polylactic acid (PLA) prepared by twin screw extrusion. *Compos Sci Technol*  
16 2010;70(12):1742-1747.
- 17 8. Rasal RM, Janorkar AV, Hirt DE. Poly (lactic acid) modifications. *Prog Polym Sci*  
18 2010;35(3):338-356.
- 19 9. Arrieta MP, López J, Hernández A, Rayón E. Ternary PLA–PHB–Limonene blends intended for  
20 biodegradable food packaging applications. *Eur Polym J* 2014;50(0):255-270.
- 21 10. Abdelwahab MA, Flynn A, Chiou B-S, Imam S, Orts W, Chiellini E. Thermal, mechanical and  
22 morphological characterization of plasticized PLA–PHB blends. *Polym Degrad Stabil*  
23 2012;97(9):1822-1828.
- 24 11. Armentano I, Bitinis N, Fortunati E, Mattioli S, Rescignano N, Verdejo R, Lopez-Manchado  
25 MA, Kenny JM. Multifunctional nanostructured PLA materials for packaging and tissue  
26 engineering. *Progr Polym Sci* 2013;38(10):1720-1747.

- 1 12. Gupta B, Revagade N, Hilborn J. Poly (lactic acid) fiber: an overview. *Progr Polym Sci*  
2 2007;32(4):455-482.
- 3 13. Herrera N, Mathew AP, Oksman K. Plasticized polylactic acid/cellulose nanocomposites  
4 prepared using melt-extrusion and liquid feeding: mechanical, thermal and optical properties.  
5 *Compos Sci Technol* 2015;106:149-155.
- 6 14. Šturcová A, Davies GR, Eichhorn SJ. Elastic Modulus and Stress-Transfer Properties of  
7 Tunicate Cellulose Whiskers. *Biomacromolecules*. 2005;6(2):1055-1061.
- 8 15. Fernandes EM, Pires RA, Mano JF, Reis RL. Bionanocomposites from lignocellulosic  
9 resources: Properties, applications and future trends for their use in the biomedical field. *Progr*  
10 *Polym Sci* 2013;38(10):1415-1441.
- 11 16. Arrieta MP, Fortunati E, Dominici F, Rayón E, López J, Kenny JM. PLA-PHB/cellulose based  
12 films: Mechanical, barrier and disintegration properties. *Polym Degrad Stabil* 2014;107(0):139-149.
- 13 17. Coccia V, Cotana F, Cavalaglio G, Gelosia M, Petrozzi A. Cellulose Nanocrystals Obtained  
14 from *Cynara Cardunculus* and Their Application in the Paper Industry. *Sustainability*  
15 2014;6(8):5252-5264.
- 16 18. Brito BSL, Pereira FV, Putaux J-L, Jean B. Preparation, morphology and structure of cellulose  
17 nanocrystals from bamboo fibers. *Cellulose* 2012;19(5):1527-1536.
- 18 19. Fortunati E, Puglia D, Luzi F, Santulli C, Kenny JM, Torre L. Binary PVA bio-nanocomposites  
19 containing cellulose nanocrystals extracted from different natural sources: Part I. *Carbohydr Polym*  
20 2013;97(2):825-836.
- 21 20. Neto WPF, Silvério HA, Dantas NO, Pasquini D. Extraction and characterization of cellulose  
22 nanocrystals from agro-industrial residue—Soy hulls. *Ind Crop Prod* 2013;42:480-488.
- 23 21 Hsieh Y-L. Cellulose nanocrystals and self-assembled nanostructures from cotton, rice straw and  
24 grape skin: a source perspective. *J Mater Sci* 2013;48(22):7837-7846.

- 1 22. Matos Ruiz M, Cavaillé JY, Dufresne A, Gérard JF, Graillat C. Processing and characterization  
2 of new thermoset nanocomposites based on cellulose whiskers. *Compos Interface* 2000;7(2):117-  
3 131.
- 4 23. Lin N, Dufresne A. Nanocellulose in biomedicine: Current status and future prospect. *Eur*  
5 *Polym J* 2014;59:302-325.
- 6 24. Cranston ED, Gray DG. Morphological and Optical Characterization of Polyelectrolyte  
7 Multilayers Incorporating Nanocrystalline Cellulose. *Biomacromolecules*. 2006;7(9):2522-2530.
- 8 25. Silvério HA, Neto WPF, Dantas NO, Pasquini D. Extraction and characterization of cellulose  
9 nanocrystals from corncob for application as reinforcing agent in nanocomposites. *Ind Crops and*  
10 *Prod* 2013;44:427-436.
- 11 26. Saïd Azizi Samir MA, Alloin F, Paillet M, Dufresne A. Tangling effect in fibrillated cellulose  
12 reinforced nanocomposites. *Macromolecules*. 2004;37(11):4313-4316.
- 13 27. Puglia D, Petrucci R, Fortunati E, Luzi F, Kenny JM, Torre L. Revalorisation of *Posidonia*  
14 *Oceanica* as Reinforcement in Polyethylene/Maleic Anhydride Grafted Polyethylene Composites. *J*  
15 *Renewable Mat* 2014;2(1):66-76.
- 16 28. Bettaieb F, Khiari R, Hassan ML, Belgacem MN, Bras J, Dufresne A, Mhenni MF, Preparation  
17 and characterization of new cellulose nanocrystals from marine biomass *Posidonia oceanica*. *Ind*  
18 *Crop Prod* 2015; doi:10.1016/j.indcrop.2014.12.038.
- 19 29. Bettaieb F, Khiari R, Dufresne A, Mhenni MF, Putaux JL, Boufi S. Nanofibrillar cellulose from  
20 *Posidoniaoceanica*: Properties and morphological features. *Ind Crop Prod* 2015;  
21 doi:10.1016/j.indcrop.2014.12.060
- 22 30. Bettaieb F, Khiari R, Dufresne A, Mhenni MF, Belgacem MN. Mechanical and thermal  
23 properties of *Posidonia oceanica* cellulose nanocrystal reinforced polymer. *Carbohydr Polym*  
24 2015;123:99-104.

- 1 31. Khiari R, Marrakchi Z, Belgacem MN, Mauret E, Mhenni F. New lignocellulosic fibres-  
2 reinforced composite materials: A stepforward in the valorisation of the *Posidonia oceanica* balls.  
3 *Compos Sci Technol* 2011;71(16):1867-1872.
- 4 32. Fortunati E, Luzi F, Puglia D, Petrucci R, Kenny JM, Torre L. Processing of PLA  
5 nanocomposites with cellulose nanocrystals extracted from *Posidonia oceanica* waste: Innovative  
6 reuse of coastal plant. *Ind Crop Prod* 2015;67:439-447.
- 7 33. Petersson L, Kvien I, Oksman K. Structure and thermal properties of poly (lactic acid)/cellulose  
8 whiskers nanocomposite materials. *Compos Sci Technol* 2007;67(11):2535-2544.
- 9 34. Liu L, Li S, Garreau H, Vert M. Selective enzymatic degradations of poly (L-lactide) and poly  
10 ( $\epsilon$ -caprolactone) blend films. *Biomacromolecules*. 2000;1(3):350-359.
- 11 35. Li S, Girard A, Garreau H, Vert M. Enzymatic degradation of polylactide stereocopolymers  
12 with predominant D-lactyl contents. *Polym Degrad Stabil* 2000;71(1):61-67.
- 13 36. Dong J, Liao L, Ma Y, Shi L, Wang G, Fan Z, Li S, Lu Z. Enzyme-catalyzed degradation  
14 behavior of l-lactide/trimethylene carbonate/glycolide terpolymers and their composites with poly  
15 (l-lactide-co-glycolide) fibers. *Polym Degrad Stabil* 2014;103:26-34.
- 16 37. Reeve MS, McCarthy SP, Downey MJ, Gross RA. Polylactide stereochemistry: effect on  
17 enzymic degradability. *Macromolecules* 1994;27(3):825-831.
- 18 38. MacDonald RT, McCarthy SP, Gross RA. Enzymatic degradability of poly (lactide): effects of  
19 chain stereochemistry and material crystallinity. *Macromolecules* 1996;29(23):7356-7361.
- 20 39. Heux L, Chauve G, Bonini C. Nonflocculating and chiral-nematic self-ordering of cellulose  
21 microcrystals suspensions in nonpolar solvents. *Langmuir*. 2000;16(21):8210-8212.
- 22 40. Fortunati E, Armentano I, Zhou Q, Iannoni A, Saino E, Visai L, Berglund LA, Kenny JM.  
23 Multifunctional bionanocomposite films of poly(lactic acid), cellulose nanocrystals and silver  
24 nanoparticles. *Carbohydr Polym* 2012;87(2):1596-1605.
- 25 41. Determination of the degree of disintegration of plastic materials under simulated composting  
26 condition in a laboratory-scale test. UN EN ISO 20200 2006.

- 1 42. Wang C-H, Fan K-R, Hsiue G-H. Enzymatic degradation of PLLA-PEOz-PLLA triblock  
2 copolymers. *Biomaterials* 2005;26(16):2803-2811.
- 3 43. Turner J, Riga A, O'Connor A, Zhang J, Collis J. Characterization of drawn and undrawn poly-  
4 L-lactide films by differential scanning calorimetry. *J Therm Anal Calorim* 2004;75(1):257-268.
- 5 44. Kale G, Kijchavengkul T, Auras R, Rubino M, Selke SE, Singh SP. Compostability of  
6 bioplastic packaging materials: an overview. *Macromol Biosci* 2007;7(3):255-277.
- 7 45. Fortunati E, Luzi F, Puglia D, Dominici F, Santulli C, Kenny JM, Torre L. Investigation of  
8 thermo-mechanical, chemical and degradative properties of PLA-limonene films reinforced with  
9 cellulose nanocrystals extracted from *Phormium tenax* leaves. *Euro Polym J* 2014;56(0):77-91.
- 10 46. Fukushima K, Abbate C, Tabuani D, Gennari M, Camino G. Biodegradation of poly (lactic  
11 acid) and its nanocomposites. *Polym Degrad Stabil* 2009;94(10):1646-1655.
- 12 47. Bitinis N, Fortunati E, Verdejo R, Bras J, Maria Kenny J, Torre L, López-Manchado MA.  
13 Poly(lactic acid)/natural rubber/cellulose nanocrystal bionanocomposites. Part II: Properties  
14 evaluation. *Carbohydr Polym* 2013;96(2):621-627.
- 15 48. Paul MA, Delcourt C, Alexandre M, Degée P, Monteverde F, Dubois P.  
16 Polylactide/montmorillonite nanocomposites: study of the hydrolytic degradation. *Polym Degrad*  
17 *Stabil* 2005;87(3):535-542.
- 18 49. Fortunati E, Peltzer M, Armentano I, Jimenez A, Kenny JM. Combined effects of cellulose  
19 nanocrystals and silver nanoparticles on the barrier and migration properties of PLA nano-  
20 biocomposites. *J Food Eng* 2013;118(1):117-124.
- 21 50. Arrieta MP, López J, Rayón E, Jiménez A. Disintegrability under composting conditions of  
22 plasticized PLA-PHB blends. *Polym Degrad Stabil* 2014; 108: 307-318.
- 23 51. Arias V, Höglund A, Odelius K, Albertsson AC. Polylactides with “green” plasticizers:  
24 Influence of isomer composition. *J Appl Polym Sci* 2013;130(4):2962-2970.

- 1 52. Khan A, Khan RA, Salmieri S, Le Tien C, Riedl B, Bouchard J, Chauve G, Tan V, Kamal MR,  
2 Lacroix M. Mechanical and barrier properties of nanocrystalline cellulose reinforced chitosan based  
3 nanocomposite films. *Carbohydr Polym* 2012;90(4):1601-1608.
- 4 53. Sanchez-Garcia MD, Lagaron JM. On the use of plant cellulose nanowhiskers to enhance the  
5 barrier properties of polylactic acid. *Cellulose* 2010;17(5):987-1004.
- 6 54. Li S, Tenon M, Garreau H, Braud C, Vert M. Enzymatic degradation of stereocopolymers  
7 derived from L-, DL- and meso-lactides. *Polym Degrad Stabil* 2000;67(1):85-90.
- 8 55. Malwela T, Ray SS. Enzymatic degradation behavior of nanoclay reinforced biodegradable  
9 PLA/PBSA blend composites. *Int J Biol Macromol* 2015;77:131-142.
- 10 56. Yamashita K, Kikkawa Y, Kurokawa K, Doi Y. Enzymatic degradation of poly (L-lactide) film  
11 by proteinase K: quartz crystal microbalance and atomic force microscopy study.  
12 *Biomacromolecules* 2005;6(2):850-857.
- 13 57. Yasuniwa M, Tsubakihara S, Sugimoto Y, Nakafuku C. Thermal analysis of the  
14 double - melting behavior of poly (L - lactic acid). *J Polym Sci Pol Phys* 2004;42(1):25-32.

15

16

## 17 **Figure and Table Captions**

18 **Figure 1:** Scheme of CNC extraction process from *Posidonia Oceanica* plant.

19 **Figure 2:** Visual observation (a) and disintegrability values (b) of PLA and PLA nanocomposites  
20 before and after different days under composting conditions.

21 **Figure 3:** FESEM investigation of PLA and PLA nanocomposites before and after 3 days in  
22 composting conditions.

23 **Figure 4:** Panel A: visual observation (a, b) of PLA and PLA nanocomposites at different times of  
24 enzymatic degradation. Panel B: weight loss at different hours (2, 6, 18 and 24 h) (c) and weight  
25 loss at different days (d) in enzymatic medium of PLA and PLA nanocomposites. (Different letters

1 in the graphs c) indicate significant statistical differences among formulations ( $p < 0.05$ ) after 24  
2 hours of test in enzymatic buffer solution).

3 **Figure 5:** Water absorption at different hours (2, 6, 18 and 24 h) (b), and water absorption at  
4 different days (c) in enzymatic medium of PLA and PLA nanocomposites. (Different letters in the  
5 graphs c) indicate significant statistical differences among formulations ( $p < 0.05$ ) after 24 hours of  
6 test in enzymatic buffer solution).

7 **Figure 6:** FESEM investigation of PLA and PLA nanocomposites after enzymatic degradation.

8 **Figure 7:** Derivative curves of weight loss for PLA and PLA nanocomposites at different  
9 enzymatic degradation times.

10 **Figure 8:** DSC thermograms at the first heating scan for PLA and PLA nanocomposites. The black  
11 curve is relative to initial time while the red/ lower curve is referred to the final time of incubation  
12 in enzymatic solution for each formulation.

13

14 **Table 1:** Thermal properties of PLA and PLA nanocomposites at different time of enzymatic  
15 degradation at the first heating scan.

16

17

Table 1

Formulations	Time	First heating						
		$T_g(^{\circ}\text{C})$	$\Delta H_{cc}(\text{J/g})$	$T_{cc}(^{\circ}\text{C})$	$\Delta H_m(\text{J/g})$	$T_m(^{\circ}\text{C})$	$T_m(^{\circ}\text{C})$	$X_c$
PLA	0 h	32.5±2.4 <sup>a</sup>	20.5±2.8 <sup>c</sup>	83.4±3.4 <sup>a</sup>	28.8±1.1 <sup>a</sup>	157.0±1.2	166.1±0.7 <sup>b</sup>	8.9±3.4 <sup>a</sup>
	2 h	39.1±0.5 <sup>b</sup>	16.0±0.3 <sup>b</sup>	80.0±0.7 <sup>a</sup>	31.9±0.5 <sup>bc</sup>	-	165.7±0.7 <sup>b</sup>	17.1±0.3 <sup>b</sup>
	6 h	50.2±0.5 <sup>c</sup>	13.0±0.6 <sup>b</sup>	89.9±0.8 <sup>b</sup>	35.2±0.7 <sup>d</sup>	-	160.9±0.9 <sup>a</sup>	21.8±0.2 <sup>b</sup>
	18 h	53.8±0.6 <sup>d</sup>	2.7±0.3 <sup>a</sup>	90.9±2.2 <sup>b</sup>	29.9±0.3 <sup>ab</sup>	-	162.2±0.4 <sup>a</sup>	29.9±0.3 <sup>c</sup>
	24 h	55.6±0.4 <sup>d</sup>	1.3±0.2 <sup>a</sup>	128.6±0.1 <sup>c</sup>	31.5±1.3 <sup>bc</sup>	-	165.0±0.5 <sup>b</sup>	32.5±1.7 <sup>cd</sup>
	2 d	58.0±1.0 <sup>e</sup>	-	-	33.0±0.8 <sup>cd</sup>	-	166.2±0.8 <sup>b</sup>	35.4±0.8 <sup>d</sup>
PLA_1CNC	0 h	35.7±2.2 <sup>a</sup>	21.6±3.6 <sup>c</sup>	85.0±1.0 <sup>a</sup>	29.6±2.9 <sup>a</sup>	156.6±1.1 <sup>a</sup>	163.5±3.0 <sup>a</sup>	8.6±3.0 <sup>a</sup>
	2 h	41.1±0.6 <sup>b</sup>	13.9±1.2 <sup>b</sup>	84.0±0.7 <sup>a</sup>	32.0±0.7 <sup>a</sup>	155.8±0.6 <sup>a</sup>	166.2±0.8 <sup>a</sup>	19.2±2.1 <sup>b</sup>
	6 h	49.1±2.0 <sup>c</sup>	13.0±0.3 <sup>b</sup>	88.9±0.8 <sup>b</sup>	33.0±0.6 <sup>a</sup>	-	165.9±0.9 <sup>a</sup>	21.3±1.0 <sup>b</sup>
	18 h	55.0±0.7 <sup>d</sup>	2.3±0.2 <sup>a</sup>	90.9±0.8 <sup>b</sup>	29.7±1.6 <sup>a</sup>	-	166.1±1.1 <sup>a</sup>	29.1±1.5 <sup>c</sup>
	24 h	60.0±0.5 <sup>e</sup>	2.5±0.1 <sup>a</sup>	90.3±0.2 <sup>b</sup>	30.7±0.2 <sup>a</sup>	-	163.3±0.8 <sup>a</sup>	30.1±0.2 <sup>c</sup>
	2 d	59.3±0.9 <sup>e</sup>	-	-	29.9±0.8 <sup>a</sup>	-	165.2±0.8 <sup>a</sup>	31.9±0.9 <sup>c</sup>
PLA_3CNC	0 h	36.6±1.8 <sup>a</sup>	22.1±3.0 <sup>c</sup>	84.9±0.1 <sup>b</sup>	29.2±1.3 <sup>b</sup>	145.4±0.6 <sup>a</sup>	157.9±0.1 <sup>a</sup>	7.5±1.7 <sup>a</sup>
	2 h	38.2±1.0 <sup>a</sup>	13.8±1.0 <sup>b</sup>	80.1±0.6 <sup>a</sup>	30.8±0.4 <sup>b</sup>	155.8±0.6 <sup>b</sup>	166.1±0.5 <sup>b</sup>	17.7±1.4 <sup>b</sup>
	6 h	44.5±1.5 <sup>b</sup>	11.2±1.0 <sup>b</sup>	80.8±1.0 <sup>a</sup>	30.8±1.1 <sup>b</sup>	-	164.9±0.6 <sup>b</sup>	20.4±0.1 <sup>b</sup>
	18 h	43.3±3.1 <sup>b</sup>	5.6±0.7 <sup>a</sup>	87.6±0.7 <sup>bc</sup>	29.2±1.0 <sup>b</sup>	-	166.0±1.1 <sup>b</sup>	20.4±0.1 <sup>c</sup>
	24 h	59.0±0.8 <sup>c</sup>	2.7±0.2 <sup>a</sup>	88.9±2.0 <sup>c</sup>	26.1±0.9 <sup>a</sup>	-	165.7±1.0 <sup>b</sup>	24.5±0.7 <sup>c</sup>
PLA_1s-CNC	0h	36.7±0.7 <sup>a</sup>	21.8±2.8 <sup>e</sup>	79.5±0.7 <sup>abc</sup>	30.8±2.6 <sup>a</sup>	-	159.9±2.8 <sup>a</sup>	9.5±0.2 <sup>a</sup>
	2h	52.7±0.6 <sup>b</sup>	14.8±0.9 <sup>d</sup>	74.8±1.0 <sup>a</sup>	30.8±0.4 <sup>a</sup>	-	165.3±0.7 <sup>b</sup>	17.0±1.4 <sup>b</sup>
	6h	52.8±1.9 <sup>b</sup>	14.9±0.5 <sup>d</sup>	76.1±0.5 <sup>ab</sup>	32.7±0.7 <sup>ab</sup>	-	165.0±0.2 <sup>b</sup>	19.0±1.3 <sup>b</sup>
	18h	52.2±0.2 <sup>b</sup>	15.0±0.6 <sup>d</sup>	76.2±1.1 <sup>ab</sup>	33.8±2.4 <sup>ab</sup>	-	164.0±0.7 <sup>b</sup>	20.1±3.2 <sup>b</sup>
	24h	55.0±0.4 <sup>cde</sup>	10.7±0.7 <sup>c</sup>	77.9±2.0 <sup>ab</sup>	34.6±0.5 <sup>ab</sup>	-	162.9±0.9 <sup>b</sup>	25.5±0.3 <sup>c</sup>
	2 d	56.5±1.5 <sup>ef</sup>	5.4±0.1 <sup>b</sup>	80.7±0.7 <sup>bc</sup>	33.5±1.6 <sup>ab</sup>	-	164.2±0.4 <sup>b</sup>	29.9±1.7 <sup>d</sup>
	3 d	54.1±0.8 <sup>bcd</sup>	5.5±0.1 <sup>b</sup>	87.0±2.3	34.5±1.8 <sup>ab</sup>	-	164.8±0.4 <sup>b</sup>	30.9±1.8 <sup>d</sup>
	5 d	54.8±0.6 <sup>bc</sup>	5.2±0.1 <sup>b</sup>	80.5±5.5 <sup>bc</sup>	35.4±1.2 <sup>b</sup>	-	163.2±1.0 <sup>b</sup>	32.2±1.4 <sup>de</sup>
	7 d	55.2±0.7 <sup>de</sup>	4.2±0.1 <sup>b</sup>	84.7±1.6 <sup>de</sup>	35.2±2.5 <sup>b</sup>	-	163.4±1.3 <sup>b</sup>	33.0±2.7 <sup>d</sup>
	8 d	55.7±0.7 <sup>de</sup>	1.5±0.5 <sup>a</sup>	90.4±2.7 <sup>e</sup>	34.1±1.3 <sup>ab</sup>	-	163.8±0.8 <sup>b</sup>	34.7±0.9 <sup>ef</sup>
	9 d	59.4±1.7 <sup>gh</sup>	-	-	34.5±1.4 <sup>ab</sup>	-	163.8±0.8 <sup>b</sup>	36.7±1.5 <sup>f</sup>
	16 d	60.2±0.4 <sup>h</sup>	-	-	34.3±1.2 <sup>ab</sup>	-	164.0±1.2 <sup>b</sup>	36.6±1.3 <sup>f</sup>
21 d	59.1±0.6 <sup>fg</sup>	-	-	33.0±3.5 <sup>ab</sup>	-	163.2±1.1 <sup>b</sup>	35.1±3.7 <sup>f</sup>	
PLA_3s-CNC	0h	39.2±1.9 <sup>a</sup>	21.3±1.3 <sup>e</sup>	82.6±0.6 <sup>bc</sup>	32.2±1.3 <sup>a</sup>	-	161.8±1.3 <sup>a</sup>	11.4±2.0 <sup>a</sup>
	2h	40.3±0.3 <sup>a</sup>	18.3±0.4 <sup>d</sup>	77.3±4.1 <sup>a</sup>	32.6±0.5 <sup>a</sup>	-	164.2±0.9 <sup>cd</sup>	15.0±0.2 <sup>b</sup>
	6h	53.4±2.2 <sup>b</sup>	16.9±2.0 <sup>cd</sup>	79.7±1.2 <sup>ab</sup>	31.5±1.4 <sup>a</sup>	-	164.7±0.6 <sup>d</sup>	15.2±0.6 <sup>b</sup>
	18h	56.7±0.3 <sup>bc</sup>	17.9±0.5 <sup>d</sup>	81.9±0.8 <sup>bc</sup>	36.7±0.2 <sup>c</sup>	-	163.2±0.1 <sup>bcd</sup>	19.6±0.3 <sup>c</sup>
	24h	54.8±0.4 <sup>b</sup>	15.6±0.1 <sup>c</sup>	81.9±0.8 <sup>bc</sup>	34.6±0.7 <sup>b</sup>	-	162.7±1.7 <sup>abc</sup>	19.8±0.6 <sup>c</sup>
	2 d	56.4±0.3 <sup>bc</sup>	13.3±0.2 <sup>b</sup>	83.0±0.5 <sup>c</sup>	37.3±0.2 <sup>c</sup>	-	163.5±0.1 <sup>bcd</sup>	25.1±0.5 <sup>d</sup>
	3 d	52.8±0.9 <sup>bc</sup>	13.2±0.1 <sup>b</sup>	82.1±0.1 <sup>bc</sup>	37.0±0.7 <sup>c</sup>	-	163.5±0.1 <sup>bcd</sup>	24.8±0.7 <sup>d</sup>
	5 d	52.7±0.7 <sup>bc</sup>	8.3±0.1 <sup>a</sup>	76.7±1.5 <sup>a</sup>	36.6±0.3 <sup>c</sup>	-	162.9±0.6 <sup>ab</sup>	29.6±0.4 <sup>e</sup>
	7 d	55.3±0.1 <sup>c</sup>	7.8±0.4 <sup>a</sup>	81.8±0.7 <sup>bc</sup>	36.1±0.9 <sup>c</sup>	-	162.9±0.6 <sup>abc</sup>	29.6±0.5 <sup>e</sup>
8 d	55.3±0.7 <sup>c</sup>	7.3±0.2 <sup>a</sup>	82.1±0.6 <sup>bc</sup>	37.4±0.2 <sup>c</sup>	-	164.0±0.7 <sup>bcd</sup>	31.3±0.5 <sup>f</sup>	

different letter in the same column indicate significant differences among formulations ( $p < 0.05$ ).

Figure 1  
[Click here to download high resolution image](#)

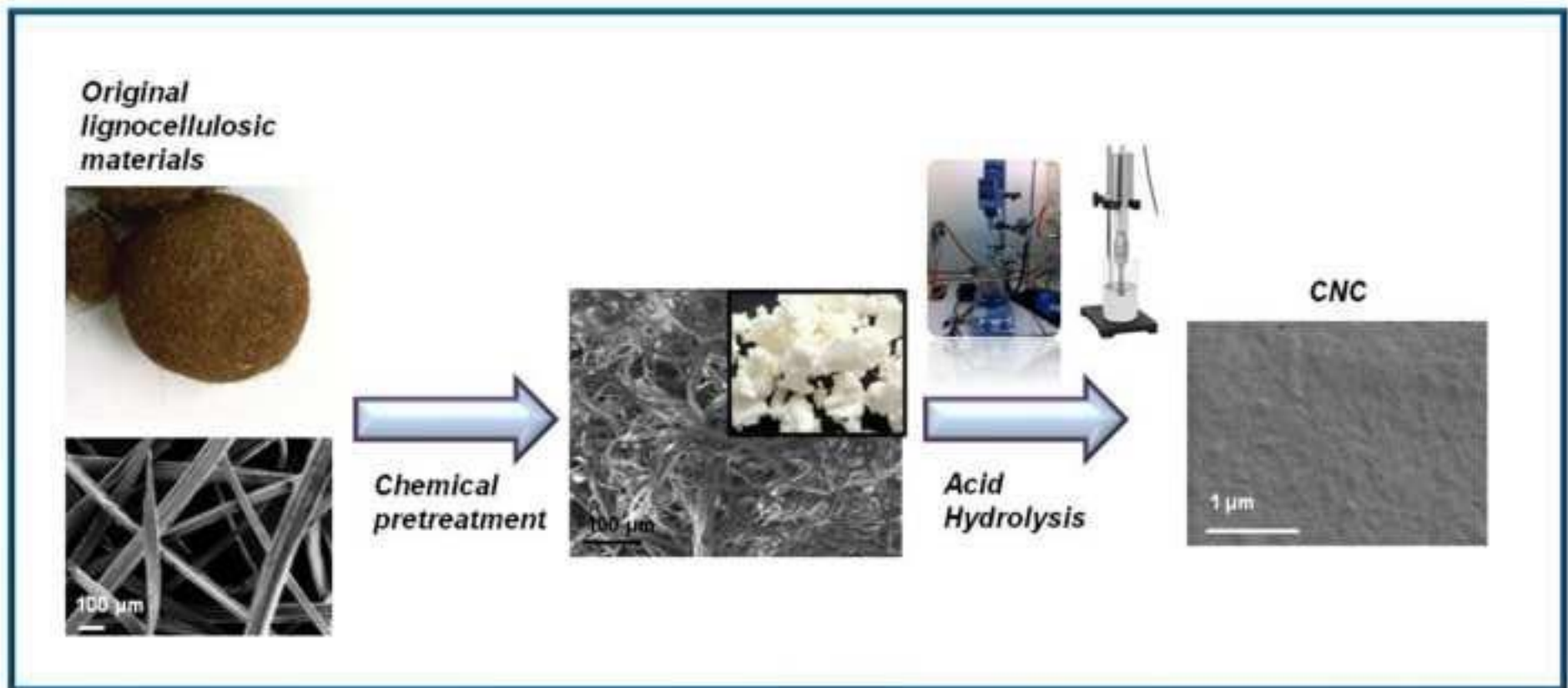


Figure 2  
[Click here to download high resolution image](#)

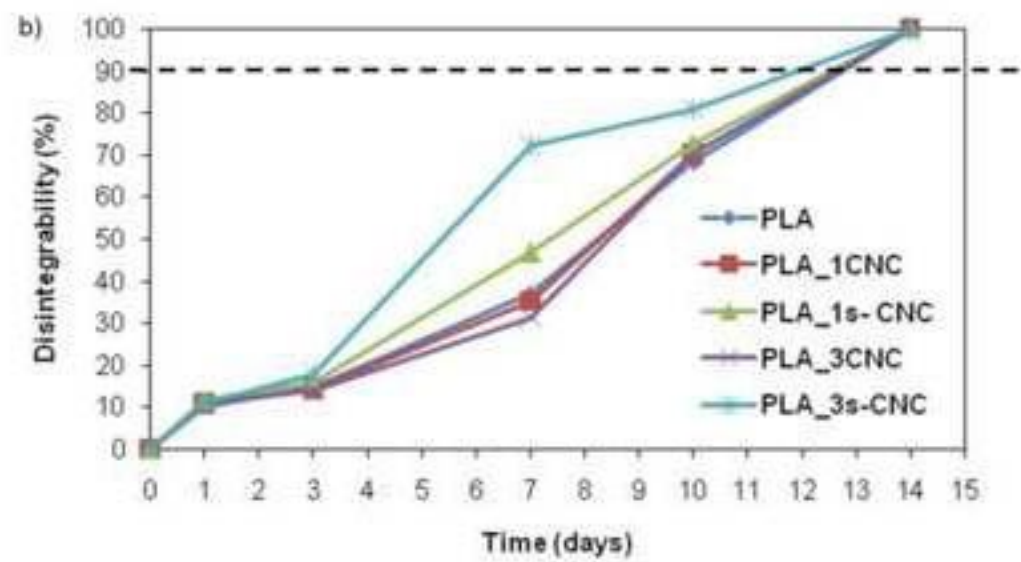
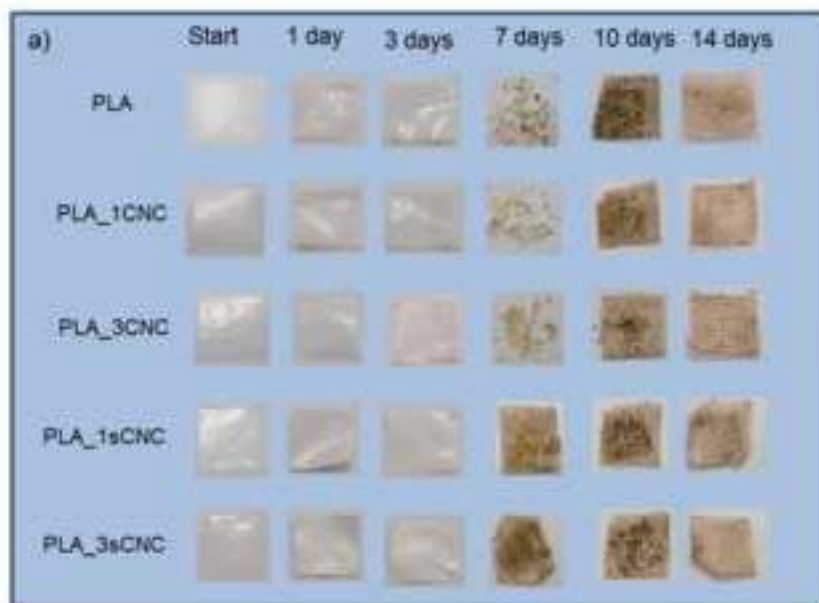


Figure 3  
[Click here to download high resolution image](#)

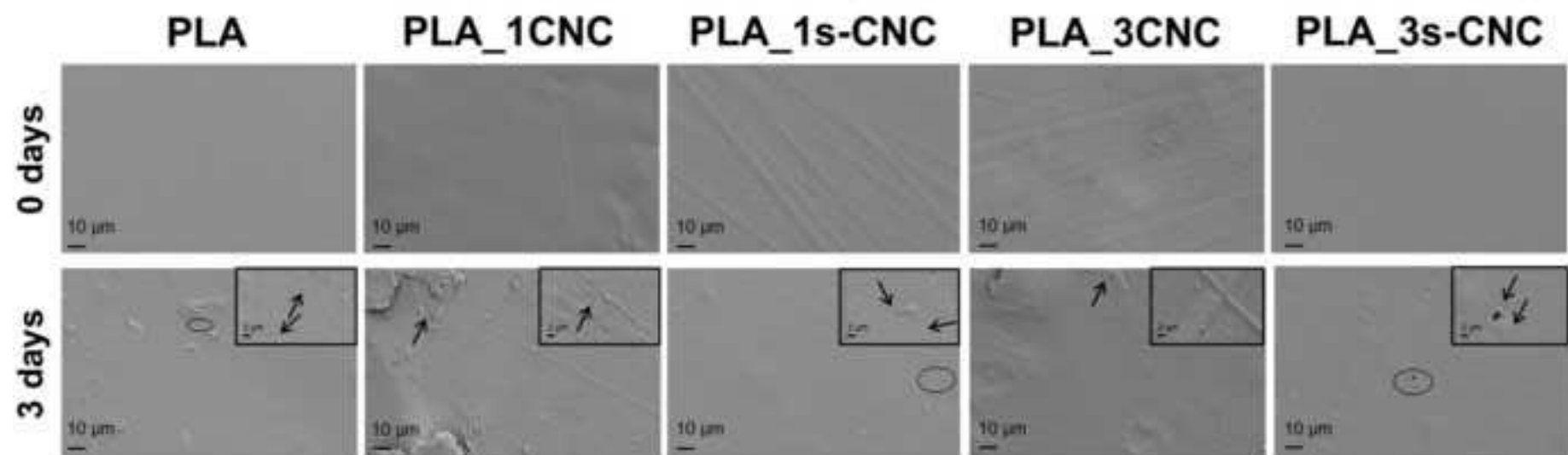
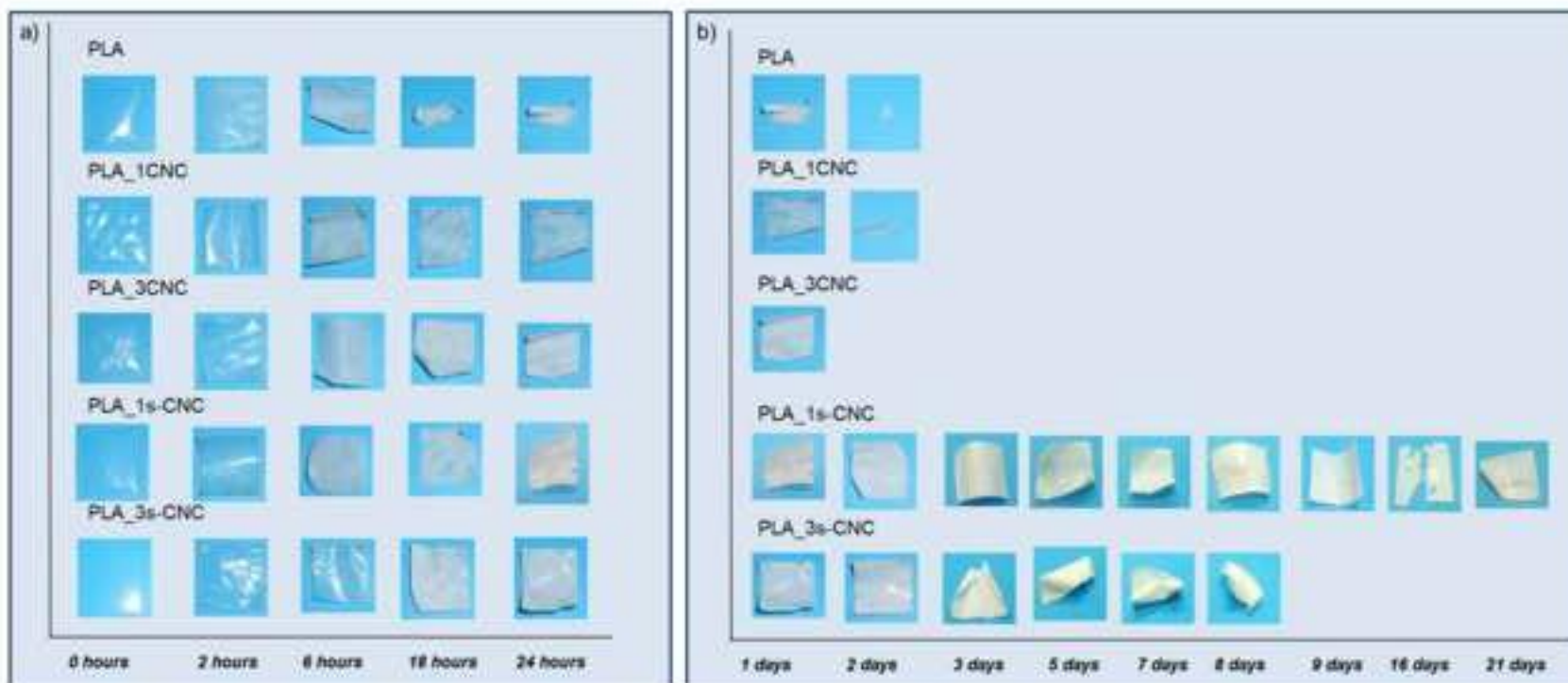


Figure 4  
[Click here to download high resolution image](#)

### Panel A



### Panel B

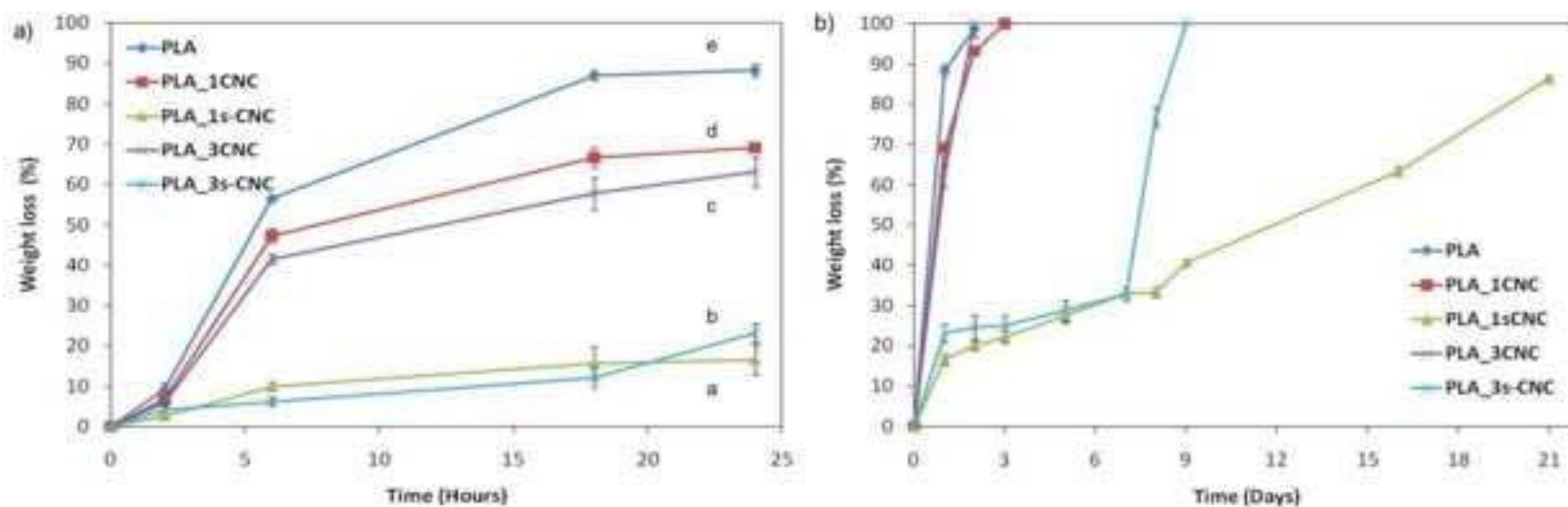


Figure 5  
[Click here to download high resolution image](#)

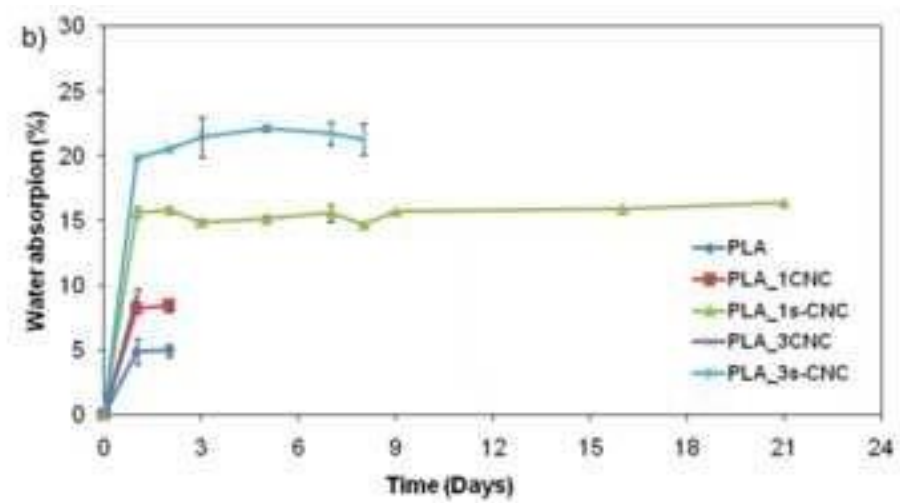
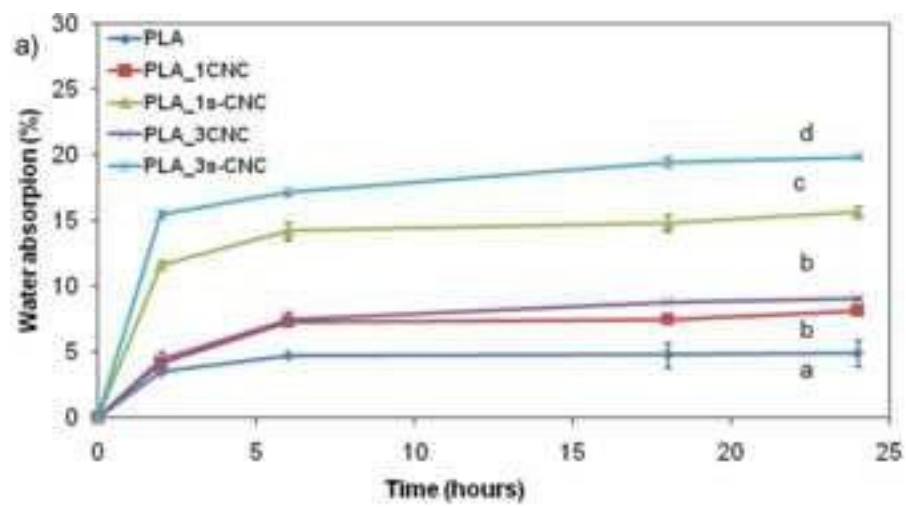


Figure 6  
[Click here to download high resolution image](#)

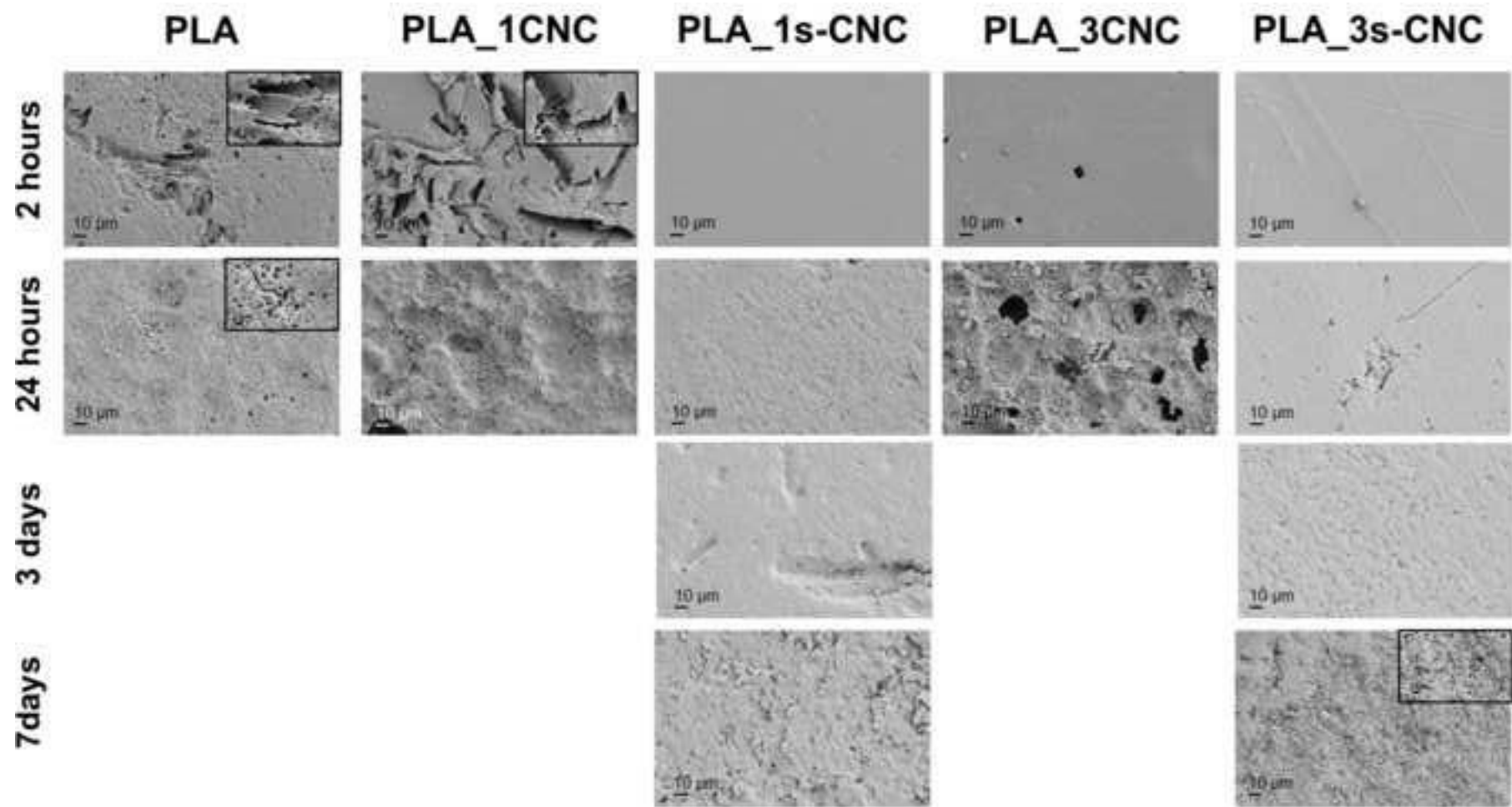


Figure 7  
[Click here to download high resolution image](#)

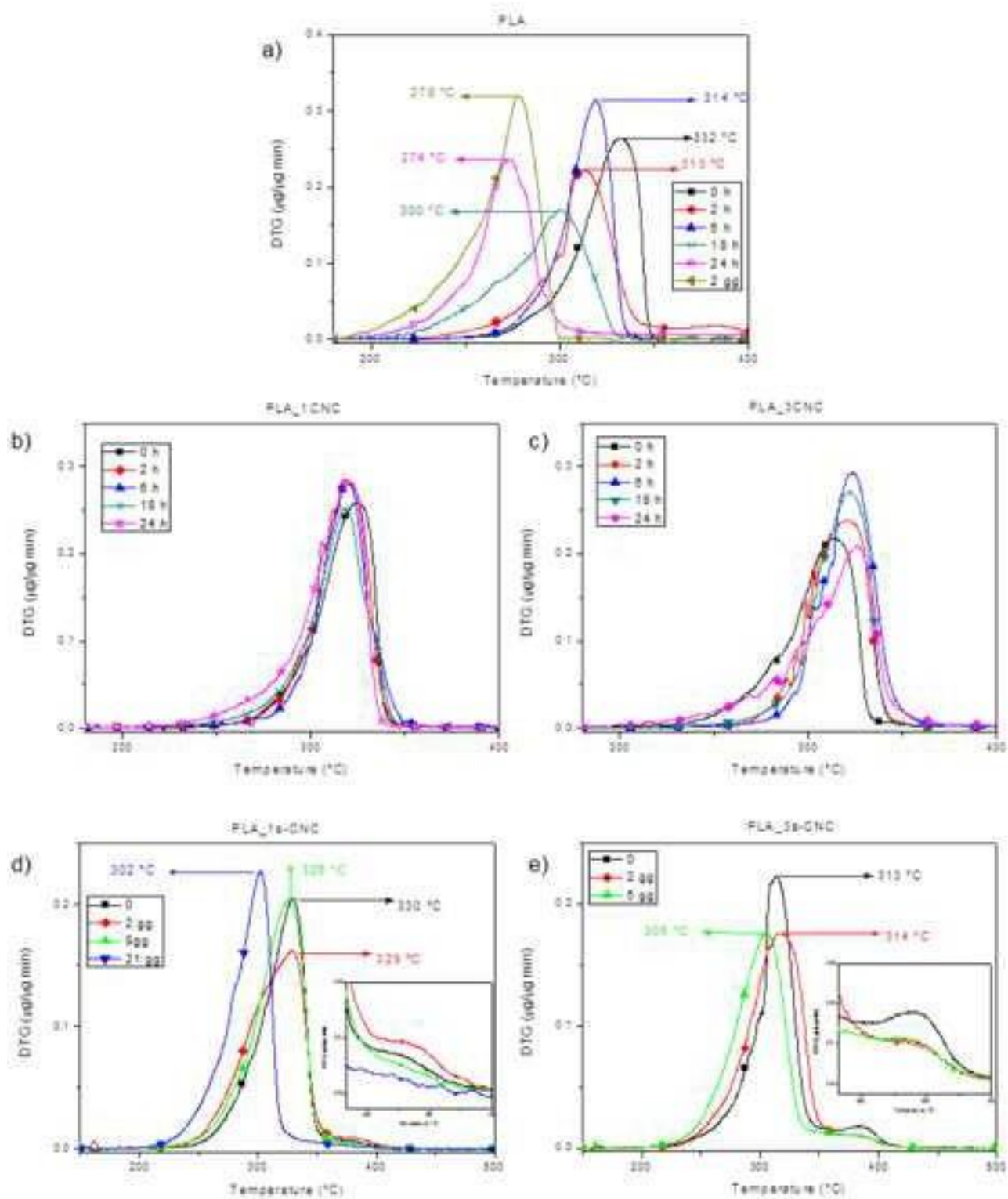


Figure 8\_New  
[Click here to download high resolution image](#)

